

# *GRID and docking analyses reveal a molecular basis for flavonoid inhibition of src-family kinase activity*

Article

Accepted Version

Wright, B., Watson, K. A. ORCID: <https://orcid.org/0000-0002-9987-8539>, McGuffin, L. J. ORCID: <https://orcid.org/0000-0003-4501-4767>, Lovegrove, J. ORCID: <https://orcid.org/0000-0001-7633-9455> and Gibbins, J. M. ORCID: <https://orcid.org/0000-0002-0372-5352> (2015) GRID and docking analyses reveal a molecular basis for flavonoid inhibition of src-family kinase activity. *Journal of Nutritional Biochemistry*, 26 (11). pp. 1156-1165. ISSN 0955-2863 doi: <https://doi.org/10.1016/j.jnutbio.2015.05.004> Available at <https://centaur.reading.ac.uk/40489/>

It is advisable to refer to the publisher's version if you intend to cite from the work. See [Guidance on citing](#).

To link to this article DOI: <http://dx.doi.org/10.1016/j.jnutbio.2015.05.004>

Publisher: Elsevier

All outputs in CentAUR are protected by Intellectual Property Rights law, including copyright law. Copyright and IPR is retained by the creators or other copyright holders. Terms and conditions for use of this material are defined in the [End User Agreement](#).

[www.reading.ac.uk/centaur](http://www.reading.ac.uk/centaur)

**CentAUR**

Central Archive at the University of Reading

Reading's research outputs online

Manuscript Number: JNB-15-50R1

Title: GRID and Docking Analyses Reveal a Molecular Basis for Flavonoid Inhibition of Src-Family Kinase Activity

Article Type: Research Article

Keywords: Flavonoid molecular templates, GRID, Sybyl docking, selective flavonoid-based analogues, kinase inhibition, flavonoid computational studies, cardiovascular disease and flavonoids, anti-platelet agents and flavonoids

Corresponding Author: Dr. Bernice Wright,

Corresponding Author's Institution: University College London

First Author: Bernice Wright

Order of Authors: Bernice Wright; Kimberly Watson; Liam McGuffin; Julie Lovegrove; Jonathan Gibbins

Abstract: Flavonoids reduce cardiovascular disease risk through anti-inflammatory, anti-coagulant and anti-platelet actions. One key flavonoid inhibitory mechanism is blocking kinase activity that drives these processes. Flavonoids attenuate activities of kinases including phosphoinositide-3-kinase (PI3K), Fyn, Lyn, Src, Syk, PKC, PIM1/2, ERK, JNK, and PKA. X-ray crystallographic analyses of kinase-flavonoid complexes show that flavonoid ring systems and their hydroxyl substitutions are important structural features for their binding to kinases. A clearer understanding of structural interactions of flavonoids with kinases is necessary to allow construction of more potent and selective counterparts.

We examined flavonoid (quercetin, apigenin and catechin) interactions with Src-family kinases (Lyn, Fyn and Hck) applying the Sybyl docking algorithm and GRID. A homology model (Lyn) was used in our analyses to demonstrate that high quality predicted kinase structures are suitable for flavonoid computational studies. Our docking results revealed potential hydrogen bond contacts between flavonoid hydroxyls and kinase catalytic site residues. Identification of plausible contacts indicated that quercetin formed the most energetically stable interactions, apigenin lacked hydroxyl groups necessary for important contacts, and the non-planar structure of catechin could not support predicted hydrogen bonding patterns. GRID analysis using a hydroxyl functional group supported docking results. Based on these findings, we predicted that quercetin would inhibit activities of Src-family kinases with greater potency than apigenin and catechin. We validated this prediction using in vitro kinase assays.

We conclude that our study can be used as a basis to construct virtual flavonoid interaction libraries to guide drug discovery using these compounds as molecular templates.

*From*

*Bernice Wright, Ph.D*

*b.wright@ucl.ac.uk*

02<sup>nd</sup> May, 2015

Dear Dr Richardson,

Please find attached a copy of the research article entitled “GRID and Docking Analyses Reveal a Molecular Basis for Flavonoid Inhibition of Src-Family Kinase Activity” for consideration for publication in *Journal of Nutritional Biochemistry*. This is original work that has not been published in any form and is not under consideration elsewhere. The manuscript has been read and approved by each author.

The mechanisms of action of flavonoids are of particular interest is their ability to function as protein and lipid kinase inhibitors. We have previously described structure-activity studies that reinforce the possibility for using flavonoid structures as templates for drug design. In the present study we examined flavonoid (quercetin, apigenin and catechin) interactions with Src-family kinases (Lyn, Fyn and Hck) using an *in silico* approach applying the Sybyl docking algorithm and GRID. We performed this study to begin clarifying our understanding of structural interactions of flavonoids with kinases to allow construction of more potent and selective counterparts derived from these compounds. Our study presents methodology that may be used to construct virtual libraries of flavonoid interactions to guide drug discovery using these compounds as molecular templates.

We would be very grateful for this work to be considered for publication in *Journal of Nutritional Biochemistry*. We look forward to hearing from you in due course.

Yours sincerely,

Bernice Wright

Research Fellow

*From*

*Bernice Wright*

*b.wright@ucl.ac.uk*

02<sup>nd</sup> May, 2015

Dear Dr. Richardson,

Please find attached a copy of the research manuscript entitled “GRID and Docking Analyses Reveal a Molecular Basis for Flavonoid Inhibition of Src-Family Kinase Activity”. We have performed a revision of our manuscript, incorporating all changes suggested by the reviewers. We thank the reviewers for their suggestions to improve the manuscript and they have been addressed as follows:

#### **Reviewer 1**

1. In the Highlights, your first point should be revised to summarize what you did, not what could be done.

We apologise for this error and we have corrected the first point in the Highlights: Docking, interaction mapping (GRID), and protein modelling methodology are used to indicate how the study of flavonoid interactions with kinases can guide drug discovery using these compounds as molecular templates.

2. The use of the term "homologous" is not quite correct on page 5, Results/Discussion.

We thank the reviewer for the thoughtful correction of the term ‘homologous’. We have replaced this term with ‘structurally similar’.

3. With regard to Figure 1, you refer to various hydroxyl positions (i.e., C-3) that are not correspondingly numbered in the figure.

We apologise for this error. We have reviewed the full manuscript and we have changed labels for hydroxyl groups to correspond with the numbering scheme in Figure 1.

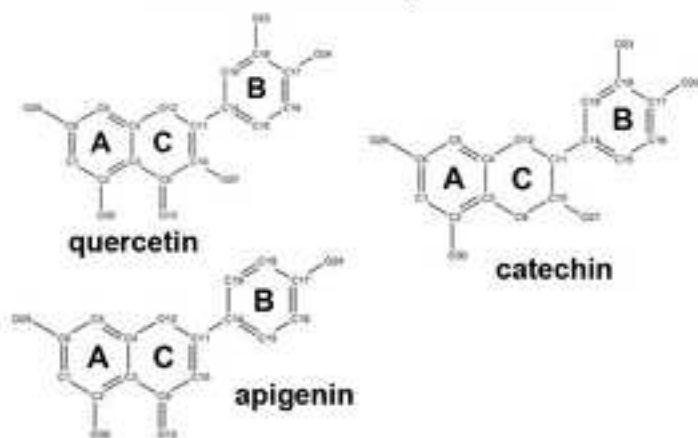
We look forward to your reply in due course.

Yours sincerely,

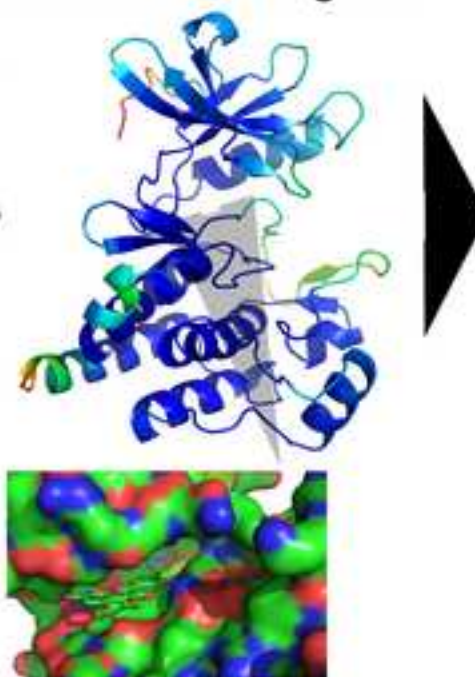
Bernice Wright

Research Fellow

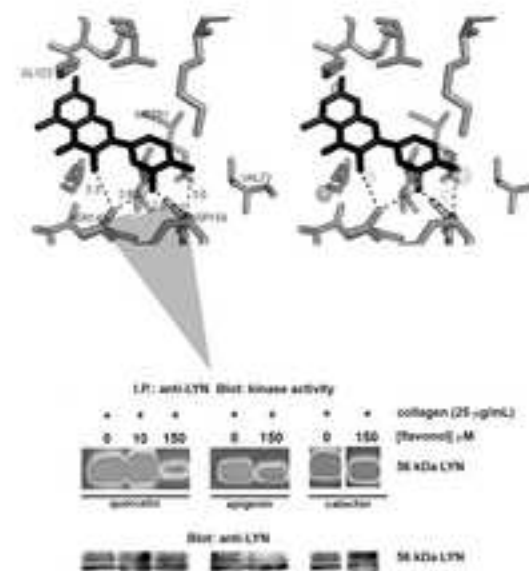
### common dietary flavonoids



### flavonoid binding to kinase ATP-binding sites



### flavonoid inhibitory binding contacts in kinase catalytic sites



## Highlights

- Docking, interaction mapping (GRID), and protein modelling methodology are used to indicate how the study of flavonoid interactions with kinases can guide drug discovery using these compounds as molecular templates.
- High quality predicted kinase structures are suitable for flavonoid computational studies.
- Structural interactions of flavonoids with kinases are necessary to allow construction of more potent and selective counterparts derived from these compounds.

1  
2  
3  
4  
5  
6  
7  
8  
9  
10  
11  
12  
13  
14  
15  
16  
17  
18  
19  
20  
21  
22  
23  
24  
25  
26  
27  
28  
29  
30  
31  
32  
33  
34  
35  
36  
37  
38  
39  
40  
41  
42  
43  
44  
45  
46  
47  
48  
49  
50  
51  
52  
53  
54  
55  
56  
57  
58  
59  
60  
61  
62  
63  
64  
65

**GRID and Docking Analyses Reveal a Molecular Basis for Flavonoid Inhibition of Src-Family Kinase Activity**

Bernice Wright<sup>1\*</sup>, Kimberly A. Watson<sup>1</sup>, Liam J. McGuffin<sup>1</sup>, Julie A. Lovegrove<sup>2</sup>, Jonathan M. Gibbins<sup>1</sup>

<sup>1</sup>Institute for Cardiovascular and Metabolic Research (ICMR), <sup>1</sup>School of Biological Sciences and <sup>2</sup>Hugh Sinclair Unit of Human Nutrition, University of Reading, Reading, RG6 6UB, Berkshire, UK

\*Corresponding Author: Bernice Wright, Institute for Cardiovascular and Metabolic Research (ICMR), School of Biological Sciences, Hopkins Building, University of Reading, Reading, Berkshire, RG6 6UB, UK Phone: +44 (0) 1183787072, Fax: +44 (0) 1183787045, Email: b.wright@reading.ac.uk

**Short Title: Molecular Basis for Flavonoid/kinase Interactions**

1  
2  
3  
4 **Abstract**  
5

6 Flavonoids reduce cardiovascular disease risk through anti-inflammatory, anti-coagulant and  
7 anti-platelet actions. One key flavonoid inhibitory mechanism is blocking kinase activity that  
8 drives these processes. Flavonoids attenuate activities of kinases including phosphoinositide-3-  
9 kinase (PI3K), Fyn, Lyn, Src, Syk, PKC, PIM1/2, ERK, JNK, and PKA. X-ray crystallographic  
10 analyses of kinase-flavonoid complexes show that flavonoid ring systems and their hydroxyl  
11 substitutions are important structural features for their binding to kinases. A clearer  
12 understanding of structural interactions of flavonoids with kinases is necessary to allow  
13 construction of more potent and selective counterparts.  
14  
15  
16  
17  
18  
19  
20  
21

22 We examined flavonoid (quercetin, apigenin and catechin) interactions with Src-family  
23 kinases (Lyn, Fyn and Hck) applying the Sybyl docking algorithm and GRID. A homology  
24 model (Lyn) was used in our analyses to demonstrate that high quality predicted kinase structures  
25 are suitable for flavonoid computational studies. Our docking results revealed potential hydrogen  
26 bond contacts between flavonoid hydroxyls and kinase catalytic site residues. Identification of  
27 plausible contacts indicated that quercetin formed the most energetically stable interactions,  
28 apigenin lacked hydroxyl groups necessary for important contacts, and the non-planar structure of  
29 catechin could not support predicted hydrogen bonding patterns. GRID analysis using a hydroxyl  
30 functional group supported docking results. Based on these findings, we predicted that quercetin  
31 would inhibit activities of Src-family kinases with greater potency than apigenin and catechin.  
32 We validated this prediction using *in vitro* kinase assays.  
33  
34  
35  
36  
37  
38  
39  
40  
41  
42  
43

44 We conclude that our study can be used as a basis to construct virtual flavonoid  
45 interaction libraries to guide drug discovery using these compounds as molecular templates.  
46  
47  
48

49 **Keywords**  
50

51 Flavonoid molecular templates, GRID, Sybyl docking, selective flavonoid-based analogues,  
52 kinase inhibition, flavonoid computational studies, cardiovascular disease and flavonoids, anti-  
53 platelet agents and flavonoids  
54  
55  
56  
57  
58  
59  
60  
61  
62  
63  
64  
65

## 1.1. Introduction

Bioactive, plant-derived flavonoids impact on the function of the vascular system through inhibition of the activity of kinases which regulate cell proliferation [1-3], the immune response [4-7], inflammatory processes [5-6], blood coagulation [8] and platelet-mediated thrombosis [9-11]. Flavonoids can achieve these effects by gaining direct access to signalling kinases in the cytosolic compartment [12-16]. A number of reports demonstrate that flavonoids are versatile and effective kinase inhibitors [1-3, 5, 7, 13, 17- 32], but they also show that these compounds are not selective. The aim of this study is to apply complementary computational methodologies to elucidate specific and important flavonoid interactions with Src-family kinases. The work demonstrates that homology models can be used for these studies together with predictive computational methodology to generate data that can guide functional studies demonstrating biological validation of predicted flavonoid interactions with kinases. This approach to screening flavonoid activities for kinases will accelerate the process of understanding the molecular interactions of flavonoids with kinases and allow translation of these compounds to more potent and selective analogues. The present study provides a basis for virtual experimental methodologies to explore structural features of these compounds, which confer selectivity and potency toward Src-family kinases.

A number of functionally-diverse kinases (myosin light chain-kinase, PKC and PKA [25]) with a central involvement in the growth, proliferation and functional maintenance of nucleated cells and key regulatory roles in signal transduction in platelets were incorporated into initial studies investigating flavonoids as molecular probes for enzyme/kinase catalytic sites. Previous reports also demonstrated that congeneric flavonoids (quercetin, catechin, apigenin) and their physiological metabolites inhibit the function of platelets by interfering with the activities of tyrosine (Syk, Fyn and Lyn) [13, 18, 30-31] and lipid (PI3K) [18] kinases, as well as phospholipases (phospholipase C $\gamma$ 2) [13, 18, 30-31]. These compounds exert pro-oxidant and antioxidant effects on the production of reactive nitrogen [32] and oxygen [33-34] species respectively, by targeting the activatory motifs of membrane-bound proteins including the FcR $\gamma$  chain [18] and Linker and Activator of T cells [18].

1  
2  
3  
4 Furthermore, studies have shown that flavonoids inhibit the activities of kinases in  
5 vascular and immune cells. Red wine polyphenolic compounds containing high levels of  
6 flavonoids inhibit the phosphorylation of serine/threonine kinases, p38 mitogen activated protein  
7 kinase (MAPK), extracellular signal-regulated kinase1/2 (ERK1/2), c-Jun N-terminal kinase and  
8 protein kinase B/Akt in vascular smooth muscle cells (VSMC) [1] and endothelial cells [3]. The  
9 phytoestrogen, genistein, was recently reported to inhibit high glucose-induced adhesion of  
10 monocytes to human aortic endothelial cells by inhibiting adenylate cyclase and protein kinase A  
11 (PKA) [5]. The flavone, luteolin was reported to inhibit VSMC proliferation by blocking the  
12 activities of Akt and Src [2]. Other flavonoid subgroups including flavanones (hesperidin,  
13 naringin) blocked high glucose-induced phosphorylation of p38 MAPK in monocytes [6]. The  
14 complex flavan-3-ol, epigallocatechin-3-gallate (EGCG) was suggested to inhibit mast cell-  
15 dependent allergic reactions *in vivo* by blocking the activities of tyrosine (Fyn, Lyn, Btk, Syk)  
16 and serine/threonine (Akt and c-Jun N-terminal kinase) kinases [7]. EGCG was also shown to  
17 reverse the progression of immune-mediated glomerulonephritis, partly by reducing oxidative  
18 stress through inhibition of inducible nitric oxide synthase, nitric oxide metabolites, p-Akt,  
19 phosphorylated ERK1/2, p47phox, and myeloperoxidase [4].  
20  
21  
22  
23  
24  
25  
26  
27  
28  
29  
30  
31  
32  
33  
34

35 These studies indicate that flavonoids interact with kinases on a molecular level, and X-  
36 ray crystallographic analyses of kinase-flavonoid complexes demonstrate that the flavonoid ring  
37 systems and their hydroxyl substitutions determine the specificity of binding of these compounds  
38 to Src-family kinases (Hck) [35], lipid kinases (PI3K $\gamma$ ) [27], serine/threonine kinases (PIM1)  
39 [24], and DNA gyrase [36]. Molecular docking analyses support such structural studies.  
40 Monomeric flavonoids were shown in docking studies to be accommodated in specific binding  
41 sites found on Raf1 kinases [28] as well as serine proteases [37] involved in blood coagulation  
42 and the inflammatory response.  
43  
44  
45  
46  
47  
48  
49  
50  
51

52 In the present study, we investigated potential binding modes (docking) and molecular  
53 interactions (GRID) of flavonoids (quercetin, apigenin and catechin: **Figure 1.**) with solved (Fyn  
54 and Hck) and modelled (Lyn) Src family kinases using GRID and docking algorithms. We  
55 suggested inhibitory potencies for these compounds based on docking and GRID data, and we  
56 authenticated these potencies using *in vitro* kinase activity assays. We report that computational  
57  
58  
59  
60  
61  
62  
63  
64  
65

1  
2  
3  
4 analysis approximating flavonoid interactions with modelled and crystallised kinases, together  
5 with biological validation, may direct and accelerate virtual screening studies for translation of  
6 these compounds into selective and potent small-molecule inhibitors applied to the discovery of  
7 therapeutic agents for vascular disorders.  
8  
9  
10

## 11 12 13 14 15 **2.1. Results/Discussion**

### 16 17 18 19 **2.1.1. The Human Lyn Kinase Model is Structurally Robust and is Structurally Similar to** 20 **the Crystal Structure of the Lyn Kinase Domain** 21

22  
23  
24 We constructed a model of the Lyn kinase domain to validate the use of homology models in our  
25 computational approach for investigating flavonoid binding within Src family kinase catalytic  
26 sites (**Figure 2.**). A model of the Lyn kinase domain was built based on the Lyn kinase domain  
27 from *Mus musculus* (PDB-ID 2h8h) template (**Figure 3A.**) using the ESyPred3D online server.  
28 The model (**Figure 3B.**) was **structurally similar** to the crystal structure of the human Lyn kinase  
29 domain (PDB-ID 3a4o) (**Figure 3C.**) - the root mean square deviation (RMSD) was 1.6 Å. The  
30 ModFOLD server (<http://www.reading.ac.uk/bioinf/ModFOLD/>) [38-39] was used to evaluate  
31 global and local model quality prior to docking.  
32  
33  
34  
35  
36  
37  
38

39 Our approach is supported by reports [40-44] describing the use of homology models for  
40 virtual screening in structure-based drug design. This methodology has been demonstrated to be  
41 reliable in accurately predicting the structure of proteins, particularly in those cases where the  
42 target is **structurally similar** to the template. Computer-aided drug design approaches can  
43 complement homology modelling approaches to provide a completely virtual environment for  
44 drug discovery. A typical structural bioinformatics workflow includes characterization of a  
45 protein target, modelling the protein using sequence homology, optimization of the protein  
46 structure and finally docking of small ligands into the active site. Previous studies have  
47 demonstrated interactions of modelled proteins with small molecules which were subsequently  
48 validated using *in vitro* biological assays. The discovery of novel PTP1B inhibitors [40], Cdc25  
49 phosphatase inhibitors [41], and angiogenin inhibitors [42] has been enabled through the use of  
50 virtual screening strategies.  
51  
52  
53  
54  
55  
56  
57  
58  
59  
60  
61  
62  
63  
64  
65

1  
2  
3  
4 For our specific problem involving the use of flavonoids as templates for drug design,  
5 high quality kinase homology models will increase the efficiency of screening because they  
6 permit the availability of a wide range of kinases. The extensive sequence information that is  
7 currently available indicates that there are an increasing number of proteins as potential drug  
8 targets with unknown structures [44]. Our approach using protein models as well as solved  
9 protein structures strengthens the possibility of screening the entire flavonoid family of  
10 compounds against all kinases that they are likely to target *in vivo*.  
11  
12  
13  
14  
15  
16  
17  
18  
19  
20

### 21 **2.1.2. Flavonoid Docking and GRID Interactions within Lyn, Fyn and Hck ATP Binding** 22 **Sites Indicate their Potencies for Inhibition of Kinase Activity** 23 24 25

26 Our previous studies demonstrated key structural differences between flavonoids for inhibition of  
27 kinase-dependent signalling in platelets [13]. In the present study, we have performed *in silico*  
28 evaluations of the binding poses (via docking using the Sybyl algorithm) and functional group  
29 interactions (via interaction energy predictions using the GRID algorithm) between quercetin,  
30 apigenin and catechin and the catalytic sites of Lyn, Fyn and Hck Src-family kinases, to examine  
31 potential underlying molecular interactions for each of these compounds and the kinases of  
32 interest. Quercetin, apigenin and catechin were manually docked into the substrate binding  
33 groove/ATP-binding site in the hinge region between the N- and C-lobes in Lyn, Fyn and Hck  
34 kinases. The Sybyl docking programme was used to predict potential interactions of the  
35 flavonoids with residues in the kinase ATP binding sites, and the GRID programme was run to  
36 predict corresponding interaction energies of hydrophilic and hydrophobic regions. The GRID  
37 programme [45] predicted three dimensional energy contour surfaces/regions (energy minima  
38 were displayed as dotted regions) within the substrate binding grooves of Hck, Fyn (crystal  
39 structures) and Lyn (homology model) corresponding to the energy minima of hydrophilic (OH)  
40 and hydrophobic (DRY) small chemical probes representative of flavonoid functional groups  
41 (OH - hydroxyl groups; DRY - aromatic rings). Used in this manner, the GRID programme was  
42 applied to independently verify the docking results. The Sybyl programme utilised a semi-  
43 flexible docking algorithm to dock the flavonoids into the ATP-binding site of the selected Src  
44 family kinases. The performance of the Sybyl algorithm [46] in ligand docking and scoring was  
45  
46  
47  
48  
49  
50  
51  
52  
53  
54  
55  
56  
57  
58  
59  
60  
61  
62  
63  
64  
65

1  
2  
3  
4 judged by its ability to reliably reproduce interactions observed for a known inhibitor-kinase  
5 complex (quercetin-Hck complex, PDB-ID 2HCK), by way of a positive control.  
6  
7

8 We extracted the X-ray pose of quercetin from within the ATP binding site of Hck (PDB-  
9 ID 2HCK - reference structure), for use as a control. Additionally, a model of quercetin was built,  
10 minimised and docked into the crystal structure of Hck. The docked pose for quercetin, from the  
11 model, superimposed onto the reference model of quercetin taken from the co-crystallised  
12 complex (**Figure 4B.**) with an RMSD of 1.372 Å, which is well within the generally accepted  
13 values of 1.5 to 2 Å. A cluster of hydrophilic interactions were observed adjacent to interactions  
14 between ASN141 and ASP154 the C ring and B ring hydroxyls in the Lyn kinase domain (**Figure**  
15 **4B.**). Modelled quercetin docked into Hck with the chromone moiety (A-C ring complex)  
16 directly adjacent to glycine (GLY344) and methionine (MET341) (**Supplemental Figure 2A.**).  
17 These data were supported by GRID, which showed areas of hydrophilic interactions (GLY344  
18 and the C ring C-10 hydroxyl) corresponding to the hydrogen bonds revealed by docking  
19 (**Supplemental Figure 2B.**). Quercetin co-crystallised with Hck [35] also formed hydrogen  
20 bonds with methionine residues (MET341). Within the ATP-binding site of Fyn (**Supplemental**  
21 **Figure 1A. and 1B.**), quercetin docked in a similar orientation as Hck; hydrogen bonds were  
22 formed between the chromone moiety and methionine (MET341) and between ASP154 and  
23 LYS39. Hydrophilic GRID interactions adjacent to MET85 were observed, and the hydrogen  
24 bond contacts formed between ASP148 and LYS39 and B ring hydroxyls were surrounded by  
25 hydrophilic GRID regions. Our published work has shown that quercetin inhibits Fyn kinase  
26 activity with high potency; the predicted pose for the flavonol, which optimises the interactions  
27 with MET85 and GLY88 may account for its potency [13]. Therefore, the predicted pose of  
28 quercetin bound to Fyn, where the chromone moiety is involved in hydrogen bond interactions,  
29 may be correlated to high potency inhibition. Within the Lyn homology model, this flavonoid  
30 docked in a similar orientation as that found in Fyn and Hck; towards asparagine and glycine  
31 residues (Lyn: ASN141, GLY23) (**Figure 5A. and 5B.**). Previous studies with fisetin [47]  
32 (bound to the active form of CDK6), have also shown that quercetin forms hydrogen bonds with  
33 the side chains of residues in the binding pocket. This binding causes large conformational  
34 changes during CDK activation by cyclin binding. The 4-keto group and the 3-hydroxyl group of  
35 fisetin are hydrogen bonded with the backbone in the hinge region between the N-terminal and C-  
36 terminal kinase domain, as has been observed for many CDK inhibitors. However, CDK2 and  
37  
38  
39  
40  
41  
42  
43  
44  
45  
46  
47  
48  
49  
50  
51  
52  
53  
54  
55  
56  
57  
58  
59  
60  
61  
62  
63  
64  
65

1  
2  
3  
4 HCK kinase in complex with other flavone inhibitors, e.g. flavopiridol, showed a different  
5 binding mode with the inhibitor rotated by about 180 degrees.  
6

7  
8 Apigenin docked within Lyn (**Figure 5C. and 5D.**), Hck (**Supplemental Figure 1C. and**  
9 **1D.**) and Fyn (**Supplemental Figure 2C. and 2D.**) with a similar number of hydrogen bonds as  
10 quercetin, suggesting that these flavonoids may inhibit Src-family kinase activity with similar  
11 potency. However, apigenin has been reported previously as a poor inhibitor of Fyn kinase  
12 activity, whilst quercetin was shown to be a high potency inhibitor [13]. It is possible that the  
13 hydrogen bond formed between the methionine (MET91: Lyn and MET341: Hck) and the para-  
14 hydroxyl in the A ring of apigenin (observed in Lyn and Hck ATP docking, but not Fyn) is  
15 necessary. GRID interactions supported the hydrogen bonds that were formed. In the Lyn kinase  
16 domain MET91 and GLU89 hydrogen bonds with the A ring C-6 hydroxyl are adjacent to  
17 favourable hydrophilic GRID regions. ASN19 binding to the A ring C-6 hydroxyl in Fyn as well  
18 as the THR82 and GLU83 bound to the B ring C-17 hydroxyl are also near favourable  
19 hydrophilic GRID regions. Within the Hck kinase domain, MET341 binds to the A ring C-6  
20 hydroxyl and SER345 and ASP348 bind to the B ring C-17 hydroxyl. Quercetin does not directly  
21 interact with methionine (MET91) in the Lyn kinase domain and, as the flavonol is a potent  
22 inhibitor of Lyn, the C ring C-10 hydroxyl must also be important. Therefore, apigenin may be  
23 less potent than quercetin due to lower affinity caused by omission of the C ring C-10 hydroxyl  
24 from the structure of the flavone. Apigenin may be more selective for Src than for Lyn, Fyn and  
25 Hck, as previous studies demonstrate; in *in vitro* pull-down assays the flavone binds Src in an  
26 adenosine triphosphate-competitive manner [48].  
27  
28  
29  
30  
31  
32  
33  
34  
35  
36  
37  
38  
39  
40  
41  
42

43 Within the ATP binding pocket of Lyn (**Figure 5E. and 5F.**), catechin docked in an  
44 opposite orientation to that of quercetin, but a similar orientation to apigenin. The B-ring of the  
45 flavan-3-ol was positioned adjacent to the methionine residue (MET91). Similar to quercetin, the  
46 C ring C-10 hydroxyl oxygen formed a hydrogen bond with the methionine (MET341) residue, in  
47 Hck (**Supplemental Figure 1E. and 1F.**) and Fyn (MET85) (**Supplemental Figure 2A. and**  
48 **2B.**). Catechin also docked with a similar number of hydrogen bonds as quercetin, in Fyn, Lyn  
49 and Hck binding sites. These data suggest that the orientation of the flavonoids within kinase  
50 ATP-binding sites rather than the number of hydrogen bonds formed may determine their  
51 inhibitory potency. Although these data suggested that catechin may inhibit Src-family kinase  
52 activity with similar high potency as quercetin, previous reports have demonstrated that this  
53  
54  
55  
56  
57  
58  
59  
60  
61  
62  
63  
64  
65

1  
2  
3  
4 compound inhibits Fyn kinase activity with low potency. GRID hydrophilic interactions  
5 corresponded to hydrogen bonds formed between GLU89, MET91 and ALA92 and A and B ring  
6 hydroxyl oxygens in the Lyn kinase domain, those formed between MET85 and C ring C-10  
7 hydroxyls in the Fyn kinase domain, and those between MET341, ALA342 and LEU273 and C  
8 and A ring hydroxyls. Therefore, although the hydroxyl groups on the non-planar C-ring form  
9 hydrogen bonds, these may not be energetically favourable. Previous studies have shown that  
10 within the ATP-binding site of DNA gyrase, epigallocatechin gallate (EGCG) a structural  
11 homologue of catechin (epicatechin), was orientated in a manner opposite to that of quercetin and  
12 a network of hydrogen bonds was formed between the flavonol and neighbouring residues but  
13 hydrogen bonds only formed between residues and the B ring of the epicatechin moiety [49].  
14 Moreover, specific knockdown of Fyn (but not Src) with small interfering RNA inhibited both  
15 EGCG-stimulated phosphorylation of Akt and endothelial nitric oxide synthase as well as  
16 production of nitric oxide in bovine aortic endothelial cells [50]. Furthermore, in an *in vitro*  
17 protein-binding assay, EGCG was found to directly bind with the GST-Fyn-SH2 domain but not  
18 the GST-Fyn-SH3 domain [51]. Therefore, complex flavan-3-ols targeted at Src homology  
19 domains may prove to be a more viable means of achieving potent inhibition of Src-family  
20 kinases than catechin.  
21  
22  
23  
24  
25  
26  
27  
28  
29  
30  
31  
32  
33  
34

35 The docking results suggest that catechin may be only partially anchored within Src-  
36 family kinase binding pockets via A-ring hydroxyl bonds, whereas quercetin and apigenin  
37 molecules with planar C rings are potentially fully anchored within these kinases. The fact that  
38 catechin is only partially anchored in the binding pocket also suggests that solvation effects may  
39 be playing a role here. The planarity of the flavonoid chromone moiety has been reported to be  
40 essential for the inhibitory activity of these compounds [13]. Therefore, quercetin and apigenin  
41 may be more potent inhibitors of Src-family kinase activity than catechin, due to more stable  
42 binding.  
43  
44  
45  
46  
47  
48  
49  
50  
51  
52  
53  
54  
55  
56  
57  
58  
59  
60  
61  
62  
63  
64  
65

### 2.1.3. Flavonoid Inhibitory Potencies for Lyn and Hck Suggested from Docked Conformations and GRID Interactions are Validated by *in vitro* Kinase Activity Assays

Quercetin inhibited the activities of Lyn and Hck to a significantly greater extent than both apigenin and catechin (**Figure 6.**). Therefore inhibitory potencies, from approximated binding conformations (docking) and functional group interactions (GRID) suggesting that quercetin was a more potent inhibitor than apigenin and catechin, were substantiated. Quercetin (150  $\mu\text{M}$ ) inhibited Hck kinase activity 9-fold greater than apigenin (150  $\mu\text{M}$ ) but only 3-fold greater than catechin (150  $\mu\text{M}$ ) (**Figure 6B. and 6C.**). Quercetin also exerted inhibition of Hck kinase activity at 10  $\mu\text{M}$ , a concentration that was achieved *in vivo* in human subjects following ingestion of a quercetin glucoside supplement. These differences indicated that C-ring hydroxylation (apigenin) may be more important than C-ring planarity (catechin) for potent inhibition of Src-family kinase activity, and the non-planar C ring C-10 hydroxyl (catechin) may elicit an inhibitory effect. Inhibition of Lyn kinase activity by quercetin was 4-fold greater than that mediated by both apigenin and catechin (**Figure 6A. and 6C.**). The differences in inhibition may be due to binding to antibodies [52] as Lyn kinase was immunoprecipitated, whereas Hck was a recombinant protein.

Recent studies show that flavonoids can bind directly to protein kinases, including Akt/protein kinase B (Akt/PKB), Fyn, Janus kinase 1 (JAK1), mitogen-activated protein kinase kinase 1 (MEK1), phosphoinositide 3-kinase (PI3K), mitogen-activated protein (MAP) kinase kinase 4 (MKK4), Raf1, and zeta chain-associated 70-kDa protein (ZAP-70) kinase, and alter their phosphorylation state to regulate multiple cell signalling pathways [53]. Apigenin, luteolin and quercetin that have been reported to inhibit GSK-3 $\beta$  [54], with 50% inhibitory values of 1.5, 1.9, and 2.0  $\mu\text{M}$ , respectively, were predicted to fit within the binding pocket of GSK-3 $\beta$  with low interaction energies (-76.4, -76.1, and -84.6 kcal $\cdot\text{mol}^{-1}$ ), respectively) and low complex energies (-718.1, -688.1, and -719.7 kcal $\cdot\text{mol}^{-1}$ ), respectively).

Previous studies have described results that are in line with those presented in the current study, as they demonstrate that flavonoid attenuation of, and binding to lipid [23, 36] and serine/threonine kinases [22-24] is dependent on a C ring C-10 hydroxyl for high potency inhibition. Substitution of the C ring C-10 hydroxyl has been shown to reduce the IC<sub>50</sub> of quercetin analogues [55]. By contrast, substitution of the C ring C-10 hydroxyl with an amine

1  
2  
3  
4 group was shown to confer greater selectivity for Src than the epidermal growth factor receptor  
5 [56]. Removal of the C ring C-10 and B ring C-16 hydroxyls (apigenin) and addition of a C-17  
6 methyl group to the B ring of quercetin (tamarixetin) correlated with low potency inhibition of  
7 Fyn involved in GPVI signalling [13]. Hydroxylation of the A ring may also be important for  
8 binding because quercetagenin (with an A ring C-1 hydroxyl that is omitted from the structure of  
9 quercetin) was demonstrated to be more potent than quercetin in the ATP binding sites of *pim*  
10 kinases [24]. Modification of A and B rings with phenol group (LY294002: analogue derivative  
11 of quercetin) on an unmodified chromone moiety also increases potency and selectivity of  
12 quercetin [57].  
13  
14

15  
16  
17  
18  
19  
20  
21 Previous docking studies of flavonoid-kinase inhibition substantiated by biological assays  
22 have also indicated that these compounds may be selective. A report described that Fyn kinase,  
23 not Lyn and Syk, was inhibited by morin in a dose-dependent manner (IC<sub>50</sub>: 5.7 μM).  
24 Kaempferol-7,4'-dimethylether was previously demonstrated as a potent p38α inhibitor,  
25 displaying 13-fold selectivity for p38α over JNK3 [58]. Flavone compounds without a 6-methoxy  
26 group preferentially inhibited JNK3; luteolin-7-O-glycoside, was identified as a potent inhibitor  
27 with the greatest selectivity toward JNK3. Flavanol compounds, however, were shown to display  
28 similar inhibitory activities toward both kinases. Delphinidin strongly inhibited TNF-alpha-  
29 induced COX-2 expression in JB6 P+ mouse epidermal (JB6 P+) cells, whereas two other major  
30 phenolic compounds (resveratrol and gallic acid) did not exert significant inhibitory effects [59].  
31 Delphinidin inhibited the TNF-alpha-induced phosphorylations of JNK, p38 MAP kinase, Akt,  
32 p90RSK, MSK1, and ERK, and subsequently blocked the activation of the eukaryotic  
33 transcription factors AP-1 and NF-κB. Kinase and pull-down assay data revealed that delphinidin  
34 inhibited Fyn kinase activity and directly bound with Fyn kinase noncompetitively with ATP  
35 [59]. This may enable us to perform pharmacophore studies with our work as a basis. A  
36 pharmacophore model for ATP-competitive inhibitors interacting with the active site of the  
37 EGFR protein tyrosine kinase, together with published X-ray crystal data of quercetin in complex  
38 with the Hck tyrosine kinase, and deschloroflavopiridol in complex with CDK2, a putative  
39 binding mode of the isoflavone genistein was previously proposed [60]. Based on literature data  
40 suggesting that a salicylic acid function, i.e. the 5-hydroxy-4-keto motif in genistein, could serve  
41 as a pharmacophore replacement of a pyrimidine ring, superposition of genistein onto the potent  
42 EGFR tyrosine kinase inhibitor 4-(3'-chlorophenylamino)-6, 7-dimethoxyquinazoline led to the  
43  
44  
45  
46  
47  
48  
49  
50  
51  
52  
53  
54  
55  
56  
57  
58  
59  
60  
61  
62  
63  
64  
65

1  
2  
3  
4 formation of 3'-chloro-5,7-dihydroxyisoflavone. This target structure was 10 times more potent  
5  
6 than genistein.  
7  
8  
9

### 10 11 **3.1. Conclusions**

12 We conclude that both computational and experimental methodologies may be used together to  
13 understand flavonoid-kinase molecular interactions. Dissections of interactions between key  
14 flavonoid functional groups and kinases have revealed important information about structural  
15 features underlying the inhibitory potencies of these compounds. Derivation of potent, selective  
16 small-molecule inhibitors from flavonoids is therefore possible. Flavonoid analogues have been  
17 constructed, but a clear understanding of the manner in which functional groups on these  
18 compounds associate with molecular targets is crucially important for substantial progress to be  
19 made in this venture.  
20  
21  
22  
23  
24  
25  
26  
27

28 We describe the basis for an organised experimental strategy based on computational  
29 guidelines that may begin to form an interaction library and help direct further design for rational  
30 screening of the flavonoid structure. Our application of complementary computational algorithms  
31 considers the inclusion of kinases with both solved structures (X-ray or NMR) and homology  
32 models to investigate the molecular interactions of key functional groups on the flavonoid  
33 structure (using GRID and docking programmes) within the Src-family kinase ATP binding site.  
34 Our method is an important pre-requisite to structure-function work that will ensure efficient  
35 dissection of the complete family of compounds within the flavonoid polyphenolic subgroup.  
36  
37  
38  
39  
40  
41  
42

43 The findings presented here form the basis for further combined computational and  
44 structural studies to fully elucidate and exploit the key molecular interactions between Src-family  
45 kinases and flavonoids. With rigorous validation of computational modelling approaches, all  
46 plausible permutations of flavonoid interactions with signalling kinases of target cells may be  
47 explored and catalogued for application to drug design.  
48  
49  
50  
51  
52  
53  
54  
55  
56  
57  
58  
59  
60  
61  
62  
63  
64  
65

## 4.1. Experimental Section

### 4.1.1. Ethics Statement

Blood was obtained from healthy aspirin-free human volunteers with written informed consent, following approval from the University of Reading Research Ethics Committee.

### 4.1.2. Materials

Quercetin, apigenin and catechin were purchased from Extrasynthese (Genay, France). Flavonoids were solubilised in dimethylsulphoxide (DMSO) obtained from Sigma (Poole, UK). Protein A Sepharose (PAS: from *Staphylococcus aureus*) and silver nitrate were also purchased from Sigma. Collagen (Type I (fibrillar) from equine tendons) was from Nycomed (Munich, Germany) and the anti-Lyn and anti-Hck primary antibodies were obtained from Santa Cruz Biotechnology (Autogen Bioclear UK Ltd; Calne, Wilts, UK). Recombinant Hck protein was obtained from New England Biolabs (Hitchin, Herts, UK). Horseradish peroxidase (HRP)-conjugated secondary antibodies were from GE Healthcare (Little Chalfont, UK). The chemiluminescence detection system was obtained from Pierce (Thermo Fisher Scientific; Rockford, IL USA). The GRID programme suite was licensed from Molecular Discovery (Perugia, Italy), the Sybyl programme was licensed from Tripos (St. Louis, USA) and the PyMOL programme was licensed from DeLano Scientific (CA, USA).

### 4.1.3. Preparation and Stimulation of Platelets

Blood was obtained from healthy, aspirin-free, human volunteers with informed consent, following approval from the University of Reading Research Ethics Committee. Platelets were isolated by differential centrifugation and suspended in modified Tyrode's-HEPES buffer (134 mM NaCl, 0.34 mM Na<sub>2</sub>HPO<sub>4</sub>, 2.9 mM KCl, 12 mM NaHCO<sub>3</sub>, 20 mM HEPES, 1 mM MgCl<sub>2</sub>, 5 mM glucose, pH 7.3) to a density of 8X10<sup>8</sup> cells·mL<sup>-1</sup> in modified Tyrode's-HEPES buffer containing 1 mM EGTA to prevent aggregation. Platelets (450 µL) were incubated with flavonoids or DMSO (1 µL: 0.2% (v/v)) for 5 min (after 10 s stirring) prior to stimulation with

1  
2  
3  
4 collagen (25  $\mu\text{g}\cdot\text{mL}^{-1}$ : 50 mL) for 90 s in an optical aggregometer at 37°C with continuous  
5  
6 stirring.  
7  
8  
9

#### 10 11 **4.1.4. Immunoprecipitation and *in vitro* Kinase Assays** 12 13 14

15 Lyn was immunoprecipitated as described previously [18]. Lyn immunoprecipitate and  
16 recombinant Hck were suspended in kinase buffer (105 mM NaCl, 20 mM HEPES (pH 7.4), 5  
17 mM  $\text{MnCl}_2$ , 5 mM  $\text{MgCl}_2$ , 2 mM NaF, 1 mM  $\text{Na}_3\text{VO}_4$ , 10  $\mu\text{M}$  adenosine triphosphate (ATP))  
18 containing 5  $\mu\text{Ci}$   $^{32}\text{P}$ -ATP per reaction, were incubated at 30°C for 20 min with flavonoids or  
19 DMSO (0.2% (v/v)) and the kinase reaction terminated through addition of an equal volume of  
20 Laemmli reducing sample treatment buffer. Proteins were separated by SDS-PAGE, and  
21 transferred to PVDF membranes which were exposed to storage phosphor screens to detect  
22 incorporation of  $^{32}\text{P}$  (autophosphorylation) into the immobilised kinase.  
23  
24  
25  
26  
27  
28  
29  
30  
31  
32

#### 33 **4.1.5. Immunoblotting** 34 35 36

37 Non-specific binding to PVDF membranes containing proteins, was blocked by incubation with  
38 5% (w/v) bovine serum albumin (BSA) dissolved in 1X Tris-buffered saline-Tween (TBS-T) (20  
39 mM Tris-base, 0.14 M NaCl, 0.1% Tween<sup>®</sup>-20; pH 7.6). Membranes were incubated with  
40 primary antibodies (1  $\mu\text{g}\cdot\text{mL}^{-1}$ ) diluted in 2% (w/v) BSA dissolved in 1X TBS-T at 4 °C  
41 overnight. Total levels of Lyn and Hck were measured by immunoblotting using anti-Lyn  
42 antibody or by silver staining (Hck). Normalisation for protein loading was performed by  
43 expressing levels of activity of Lyn and Hck, relative to total levels of those proteins, and was  
44 expressed as a percentage compared to the untreated control that represented 100% activity. For  
45 immunoblotting, blots were washed for 45 min in 1X TBS-T before incubation with a HRP-  
46 conjugated secondary antibody (1:4000 dilution) for 2 h at room temperature (RT) with rotation.  
47  
48  
49  
50  
51  
52  
53  
54  
55  
56  
57  
58  
59  
60  
61  
62  
63  
64  
65

1  
2  
3  
4 BioRad GS710 densitometer with Quantity One analysis software (BioRad; Hemel Hempstead,  
5  
6 UK).

#### 11 **4.1.6. Structural Alignments**

14  
15 The Dali-lite structural sieving server was used to perform structural alignments of Lyn, Fyn and  
16 Hck kinase domains. This server generates structural alignments by an iterative process involving  
17 filtering out residue-residue correspondences until optimal (superimposable) corresponding  
18 residues are achieved in structures, under a threshold of RMSD. The lsqkab programme in the  
19 CCP4 programme suite was used to perform structural alignments of the crystallised and docked  
20 quercetin molecules.  
21  
22  
23  
24  
25  
26  
27  
28  
29

#### 30 **4.1.7. Homology Modelling**

31  
32  
33 Homology models were built for Lyn tyrosine kinase (Homo sapiens) from the Src kinase crystal  
34 structure template (PDB ID: 2H8H) using ESyPred3D server [61]. The per-residue error was  
35 predicted using the ModFOLD server [38, 62-63]. The colour-coding used by ModFOLD  
36 represents the residue accuracy according to a pseudo-temperature scheme (blue indicates  
37 residues closest to the native structure; red, those furthest from the native structure). Residues  
38 coloured in red are also predicted to have a higher propensity for flexibility according to the  
39 DISOclust method [64]. Images were rendered using PyMOL (<http://www.pymol.org>).  
40  
41  
42  
43  
44  
45  
46  
47  
48  
49

#### 50 **4.1.8. GRID Analysis**

51  
52  
53 The GRID programme [45] was utilised to predict potential binding sites, represented as three  
54 dimensional energy contour surfaces (or regions), for functional groups within the ATP binding  
55 pocket of Hck, Fyn (crystal structures) and Lyn (homology model) kinase domains. The resulting  
56 energy contours indicate the location of energetically favourable interactions, with negative  
57  
58  
59  
60  
61  
62  
63  
64  
65

1  
2  
3  
4 energy levels indicating favourable regions. The potential energy ( $E_{xyz}$ ) between the target (Hck,  
5 Fyn or Lyn) and a small chemical probe (OH, OH<sub>2</sub> and DRY) at each node of the GRID was  
6 calculated as:  $E_{xyz} = \Sigma E_{EL} + \Sigma E_{HB} + \Sigma E_{LJ}$  [47, 66].  $\Sigma E_{EL}$  is defined as the appropriately modified  
7 electrostatic energy,  $\Sigma E_{HB}$  is the hydrogen bonding energy and  $\Sigma E_{LJ}$  is the Lennard-Jones  
8 potential energy between probe and target atoms. Successive probe positions were sampled in the  
9 same way until each grid point was assigned an energy value. The program GRIN, the first step  
10 in the GRID calculation, was used to prepare each of the coordinate files by removing hydrogens  
11 (in the case of the Lyn homology model) adding counterions ( $Na^+$  was used in each case) to  
12 neutralise the overall charge on the protein taking care not to include counterions near any  
13 potential binding sites and including the associated energy variables to individual atom types as  
14 defined in GRIN. The move directive in GRID was set to -1 to allow the counterions to move in  
15 response to the probe. The GRID calculations were performed using a grid spacing of 0.5Å in a  
16 GRID box defined as a three dimensional grid of points around and within the ATP binding  
17 pocket of Hck, Fyn or Lyn (approximately X x Y x Z). Hydrophilic (OH) and hydrophobic  
18 (DRY) probes were selected as being most representative of flavonoid functional groups (OH -  
19 hydroxyl groups; DRY - aromatic rings), although, additional chemical probes used included O,  
20 OFU, hydrogen donor: OH<sub>2</sub>, OH, hydrophobic: DRY and hydrogen acceptor: N1+, N1, N:=, O-  
21 (default) probes. The program MINIM was used convert the GRID output to a readable format  
22 suitable for input to PyMOL (DeLano Scientific) for graphical viewing and interpretation.  
23  
24  
25  
26  
27  
28  
29  
30  
31  
32  
33  
34  
35  
36  
37  
38  
39  
40  
41  
42

#### 43 **4.1.9. Docking Analysis**

44  
45  
46 The crystal structures of Fyn (2DQ7) and Hck (2HCK) were obtained from the protein data bank  
47 (<http://www.ebi.ac.uk>). In order to prepare the protein structures for the docking experiments  
48 duplicate chains, where present, as well as all water molecules were removed. Additionally, all  
49 ligands were extracted from the coordinate files. Finally, the protein structures were prepared for  
50 the docking runs using the Biopolymer Structure Preparation Tool implemented in the  
51 programme SYBYL. Docking experiments utilized the Surflex-Dock automatic docking  
52 algorithm. The structures of quercetin, apigenin and catechin were built using the BUILDER  
53 module in InsightII and a conformational minimisation was performed for these ligands using the  
54  
55  
56  
57  
58  
59  
60  
61  
62  
63  
64  
65

1  
2  
3  
4 consistent valence force field (CVFF) to the lowest energy conformers for docking analyses.  
5  
6 Docking was performed by placing the molecule in the binding pocket of the protein (together in  
7  
8 one pdb file) before proceeding with the docking algorithm. In order to calculate the hydrogen  
9  
10 bond (H-bond), van der Waals (vdW) and hydrophobic interactions, the resulting PDB files from  
11  
12 the docking runs were input to the program CONTACTS, available in the CCP4 programme  
13  
14 suite. Potential H-bonds were assigned if the distance between two electronegative atoms was  
15  
16 less than 3.3 Å, whereas any separation greater than 3.3 Å, but less than 4.0 Å, was considered a  
17  
18 vdW interaction.  
19  
20  
21  
22  
23  
24  
25  
26  
27  
28  
29  
30  
31  
32  
33  
34  
35  
36  
37  
38  
39  
40  
41  
42  
43  
44  
45  
46  
47  
48  
49  
50  
51  
52  
53  
54  
55  
56  
57  
58  
59  
60  
61  
62  
63  
64  
65

## 5.1. References

1. Oak MH, Chataigneau M, Keravis T, Chataigneau T, Beretz A et al. Red wine polyphenolic compounds inhibit vascular endothelial growth factor expression in vascular smooth muscle cells by preventing the activation of the p38 mitogen-activated protein kinase pathway. *Arterioscler Thromb Vasc Biol* 2003; 23: 1001-1007.
2. Lang Y, Chen D, Li D, Zhu M, Xu T et al. Luteolin inhibited hydrogen peroxide-induced vascular smooth muscle cells proliferation and migration by suppressing the Src and Akt signalling pathways. *J Pharm Pharmacol* 2012; 64: 597-603.
3. Kobuchi H, Roy S, Sen CK, Nguyen HG and Packer L. Quercetin inhibits inducible ICAM-1 expression in human endothelial cells through the JNK pathway. *Am J Physiol* 1999; 277: C403-C411.
4. Peng A, Ye T, Rakheja D, Tu Y, Wang T et al. The green tea polyphenol (-)-epigallocatechin-3-gallate ameliorates experimental immune-mediated glomerulonephritis. *Kidney Int* 2011; 80: 601-611.
5. Babu PV, Si H, Fu Z, Zhen W and Liu D Genistein prevents hyperglycemia-induced monocyte adhesion to human aortic endothelial cells through preservation of the cAMP signaling pathway and ameliorates vascular inflammation in obese diabetic mice. *J Nutr* 2012; 142: 724-730.
6. Wu CH, Wu CF, Huang HW, Jao YC and Yen GC Naturally occurring flavonoids attenuate high glucose-induced expression of proinflammatory cytokines in human monocytic THP-1 cells. *Mol Nutr Food Res* 2009; 53: 984-995.
7. Maeda-Yamamoto M, Inagaki N, Kitaura J, Chikumoto T, Kawahara H et al. *O*-methylated catechins from tea leaves inhibit multiple protein kinases in mast cells. *J Immunol* 2004; 172: 4486-4492.
8. Bucki R, Pastore JJ, Giraud F, Sulpice JC and Janmey PA Flavonoid inhibition of platelet procoagulant activity and phosphoinositide synthesis. *J Thromb Haemost* 2003; 1: 1820-1828.
9. Briggs WH, Folts JD, Osman HE and Goldman IL Administration of raw onion inhibits platelet-mediated thrombosis in dogs. *J Nutr* 2001; 131: 2619-2622.

- 1  
2  
3  
4 10. Navarro-Nuñez L, Lozano ML, Palomo M, Martinez C, Vicente V et al. Apigenin inhibits  
5  
6 platelet adhesion and thrombus formation and synergises with aspirin in the suppression  
7  
8 of the arachidonic acid pathway. *J Agric Food Chem* 2008; 56: 2970-2976.  
9
- 10  
11 11. Sano T, Oda E, Yamashita T, Naemura A, Ijiri Y, et al. Anti-thrombotic effect of  
12  
13 proanthocyanidin, a purified ingredient of grape seed. *Thromb Res* 2005; 115: 115-121.  
14
- 15  
16 12. Pawlikowska-Pawlega B, Gruszecki WI, Misiak L, Paduch R, Piersiak T, et al.  
17  
18 Modification of membranes by quercetin, a naturally occurring flavonoid, via its  
19  
20 incorporation into the polar head group. *Biochim Biophys Acta* 2007; 1768: 2195-2204.  
21
- 22  
23 13. Wright B, Moraes LA, Kemp CF, Mullen W, Crozier A et al. A structural basis for the  
24  
25 inhibition of collagen-stimulated platelet function by quercetin and structurally related  
26  
27 flavonoids. *Br J Pharmacol* 2010; 159: 1312-1325.  
28
- 29  
30 14. Wright B, Gibson T, Spencer J, Lovegrove JA and Gibbins JM Platelet-mediated  
31  
32 metabolism of the common dietary flavonoid, quercetin. *PLoS One* 2010; 5: e9673.  
33
- 34  
35 15. Gryglewski RJ, Korbut R, Robak J and Swies J On the mechanism of antithrombotic  
36  
37 action of flavonoids. *Biochem Pharmacol* 1987; 36: 317-322.  
38
- 39  
40 16. Fiorani M, Accorsi A and Cantoni O Human red blood cells as a natural flavonoid  
41  
42 reservoir. *Free Rad Res* 2003; 37: 1331-1338.  
43
- 44  
45 17. Lill G, Voit S, Schror K and Weber AA Complex effects of different green tea catechins  
46  
47 on human platelets. *FEBS Lett* 2003; 546: 265-270.  
48
- 49  
50 18. Hubbard GP, Stevens JM, Cicmil M, Sage T, Jordan PA et al. Quercetin inhibits collagen-  
51  
52 stimulated platelet activation through inhibition of multiple components of the  
53  
54 glycoprotein VI signalling pathway. *J Thromb Haemost* 2003; 1: 1079-1088.  
55
- 56  
57 19. Zhang Y, Han G, Fan B, Zhou Y, Zhou X et al. Green tea (-)-epigallocatechin-3-gallate  
58  
59 down-regulates VASP expression and inhibits breast cancer cell migration and invasion  
60  
61 by attenuating Rac1 activity. *Eur J Pharmacol* 2009; 606: 172-179.  
62
- 63  
64 20. Peluso MR. Flavonoids attenuate cardiovascular disease, inhibit phosphodiesterase, and  
65  
66 modulate lipid homeostasis in adipose tissue and liver. *Exp Biol Med* 2006; 231: 1287-  
1299.

- 1  
2  
3  
4 21. Deana R, Turetta L, Donella-Deana A, Donà M, Brunati AM et al. Green tea  
5 epigallocatechin-3-gallate inhibits platelet signalling pathways triggered by both  
6 proteolytic and non-proteolytic agonists. *Thromb Haemost* 2003; 89: 866–874.  
7  
8  
9  
10 22. Agullo G, Gamet-Payrastre L, Manenti S, Viala C, Remesy C et al. Relationship between  
11 flavonoids structure and inhibition of phosphatidylinositol 3-kinase: A comparison with  
12 tyrosine kinase and protein kinase C inhibition. *Biochem Pharmacol* 1997; 53: 1649-  
13 1657.  
14  
15  
16  
17  
18 23. Gamet-Payrastre L, Manenti S, Gratacap MP, Tulliez J, Chap H et al. Flavonoids and the  
19 inhibition of PKC and PI 3-kinase. *Gen Pharmacol* 1999; 32: 279-286.  
20  
21  
22 24. Holder S, Zemskova M, Zhang C, Tabrizizad M, Bremer R et al. Characterisation of a  
23 potent and selective small-molecule inhibitor of the PIM1 kinase. *Mol Cancer Ther* 2007;  
24 6: 163-172.  
25  
26  
27  
28 25. Hagiwara M, Inoue S, Tanaka T, Nunoki K, Ito M et al. Differential effects of flavonoids  
29 as inhibitors of tyrosine protein kinases and serine/threonine protein kinases. *Biochem*  
30 *Pharmacol* 1988; 37: 2987-2992.  
31  
32  
33  
34 26. Cochet C, Feige JJ, Pirollet F, Keramidas M and Chambaz EM Selective inhibition of a  
35 cyclic nucleotide independent protein kinase (G-type casein kinase) by quercetin and  
36 related polyphenols. *Biochem Pharmacol* 1982; 31: 157-1361.  
37  
38  
39  
40 27. Walker EH, Pacold ME, Perisic O, Stephens L, Hawkins PT et al. Structural determinants  
41 of phosphoinositide 3-kinase inhibition by wortmannin, LY294002, quercetin, myricetin  
42 and staurosporine. *Mol Cell* 2000; 6: 909-919.  
43  
44  
45  
46 28. Jung SK, Lee KW, Kim HY, Oh MH, Byun S, et al. Myricetin suppresses UVB-induced  
47 wrinkle formation and MMP-9 expression by inhibiting Raf. *Biochem Pharmacol* 2010;  
48 79: 1455-1461.  
49  
50  
51  
52 29. Davies SP, Reddy H, Caivano M and Cohen P Specificity and mechanism of action of  
53 some commonly used protein kinase inhibitors. *Biochem J* 2000; 351: 95-105.  
54  
55  
56  
57 30. Hubbard GP, Wolfram S, Lovegrove JA and Gibbins JM Ingestion of quercetin inhibits  
58 platelet aggregation and essential components of the collagen-stimulated platelet  
59 activation pathway in humans. *J Thromb Haemost* 2004; 2: 2138-2145.  
60  
61  
62  
63  
64  
65

- 1  
2  
3  
4 31. Hubbard GP, Wolffram S, Gibbins JM and Lovegrove JA Ingestion of onion soup high in  
5 quercetin inhibits platelet aggregation and essential components of the collagen-  
6 stimulated platelet activation pathways in man: A pilot study. *Br J Nutr* 2006; 96: 482-  
7 488.  
8  
9  
10  
11 32. Freedman JE, Parker C, Li L, Perlman JA, Frei B, et al. Select flavonoids and whole juice  
12 from purple grapes inhibit platelet function and enhance nitric oxide release. *Circulation*  
13 2001; 103: 2792-2798.  
14  
15  
16  
17 33. Pignatelli P, Ghiselli A, Buchetti B, Carnevale R, Natella F et al. Polyphenols  
18 synergistically inhibit oxidative stress in subjects given red and white wine. *Atheroscler*  
19 2006; 188: 77-83.  
20  
21  
22  
23 34. Pignatelli P, Pulcinelli FM, Celestini A, Lenti L, Ghiselli A, et al. The flavonoids  
24 quercetin and catechin synergistically inhibit platelet function by antagonizing the  
25 intracellular production of hydrogen peroxide. *Am J Clin Nutr* 2000; 72: 1150-1155.  
26  
27  
28  
29 35. Sicheri F, Moarefi I and Kuriyan J. Crystal structure of the Src family tyrosine kinase  
30 Hck. *Nature* 1997; 385: 602-609.  
31  
32  
33 36. Plaper A, Golob M, Hafner I, Oblak M, Solmajer T et al. Characterization of quercetin  
34 binding site on DNA gyrase. *Biochem Biophys Res Commun* 2003; 306: 530-536.  
35  
36  
37 37. Cuccioloni M, Mozzicafreddo M, Bonfili L, Cekarini V, Eleuteri AM, et al. Natural  
38 occurring polyphenols as template for drug design. Focus on serine proteases. *Chem Biol*  
39 *Drug Des* 2009; 74: 1-15.  
40  
41  
42  
43 38. McGuffin LJ, Buenavista MT and Roche DB The ModFOLD4 server for the quality  
44 assessment of 3D protein models. *Nucleic Acids Res* 2013; doi: 10.1093/nar/gkt294.  
45  
46  
47 39. Pettitt CS, McGuffin LJ and Jones DT Improving sequenced based fold recognition by  
48 use of 3D model quality assessment. *Bioinformatics* 2005; 21: 3509-3515.  
49  
50  
51 40. Park H, Bhattarai BR, Ham SW and Cho H Structure-based virtual screening approach to  
52 identify novel classes of PTP1B inhibitors. *Eur J Med Chem* 2009; 44: 3280-3284.  
53  
54  
55 41. Park H, Li M, Choi J, Cho H and Ham SW Structure-based virtual screening approach to  
56 identify novel classes of Cdc25B phosphatase inhibitors. *Bioorg Med Chem Lett* 2009;  
57  
58  
59  
60  
61  
62  
63  
64  
65

- 1  
2  
3  
4 19: 4372-4375.  
5  
6  
7 42. Howlin BJ, Tomkinson NP, Chen J and Webb GA Design of potential angiogenin  
8 inhibitors. *J Comput Aided Mol Des* 1994; 8: 223-230.  
9  
10 43. Ahmed A, Choo H, Cho YS, Park WK and Pae AN Identification of novel serotonin 2C  
11 receptor ligands by sequential virtual screening. *Bioorg Med Chem* 2009; 17: 4559-4568.  
12  
13 44. Takeda-Shitaka M, Takaya D, Chiba C, Tanaka H and Umeyama H Protein structure  
14 prediction in structure based drug design. *Curr Med Chem* 2004; 11: 551-558.  
15  
16 45. Goodford, P. J. A computational procedure for determining energetically favorable  
17 binding sites on biologically important macromolecules. *J Med Chem* 1985; 28: 849-857.  
18  
19 46. Hevener KE, Zhao W, Ball DM, Babaoglu K, Qi J et al. Validation of molecular docking  
20 programs for virtual screening against dihydropteroate synthase. *J Chem Inf Model* 2009;  
21 49: 444-460.  
22  
23 47. Lu H, Chang DJ, Baratte B, Meijer L and Schulze-Gahmen U Crystal structure of a  
24 human cyclin-dependent kinase 6 complex with a flavonol inhibitor, fisetin. *J Med Chem*  
25 2005; 48: 737-743.  
26  
27 48. Byun S, Park J, Lee E, Lim S, Yu JG et al. Src kinase is a direct target of apigenin against  
28 UVB-induced skin inflammation. *Carcinogenesis* 2012; 34: 397-405.  
29  
30 49. Gradisar H, Pristovsek P, Plaper A, Jerala R. Green tea catechins inhibit bacterial DNA  
31 gyrase by interaction with its ATP binding site. *J Med Chem* 2007; 50: 264-271.  
32  
33 50. Kim JA, Formoso G, Li Y, Potenza MA, Marasciulo FL. et al. Epigallocatechin gallate, a  
34 green tea polyphenol, mediates NO-dependent vasodilation using signaling pathways in  
35 vascular endothelium requiring reactive oxygen species and Fyn. *J Biol Chem* 2007; 282:  
36 13736-13745.  
37  
38 51. He Z, Tang F, Ermakova S, Li M, Zhao Q. et al. Fyn is a novel target of (-)-  
39 epigallocatechin gallate in the inhibition of JB6 C141 cell transformation. *Mol Carcinog*  
40 2008; 47: 172-183.  
41  
42 52. Liu YC, Yang ZY, Du J, Yao XJ, Lei RX et al. Study of the interactions of kaempferol  
43 and quercetin with intravenous immunoglobulin by fluorescence quenching, fourier  
44  
45  
46  
47  
48  
49  
50  
51  
52  
53  
54  
55  
56  
57  
58  
59  
60  
61  
62  
63  
64  
65

- 1  
2  
3  
4 transformation infrared spectroscopy and circular dichroism spectroscopy. Chem Pharm  
5 Bull (Tokyo) 2008; 56: 443-45.  
6  
7  
8  
9 53. Hou DX and Kumamoto T Flavonoids as protein kinase inhibitors for cancer  
10 chemoprevention: direct binding and molecular modeling. Antioxid Redox Signal 2010;  
11 13: 691-719.  
12  
13  
14 54. Johnson JL, Rupasinghe SG, Stefani F, Schuler MA, Gonzalez de Mejia E Citrus  
15 flavonoids luteolin, apigenin, and quercetin inhibit glycogen synthase kinase-3 $\beta$   
16 enzymatic activity by lowering the interaction energy within the binding cavity. J Med  
17 Food 2011; 14: 325-333.  
18  
19  
20 55. Matter WF, Brown RF and Vlahos CJ The inhibition of phosphatidylinositol 3-kinase by  
21 quercetin and analogs. Biochem Biophys Res Comm 1992; 186: 624-631.  
22  
23  
24 56. Huang H, Jia Q, Ma J, Qin G, Chen Y et al. Discovering novel quercetin-3-O-amino acid-  
25 esters as a new class of Src tyrosine kinase inhibitors. Eur J Med Chem 2009; 44: 1982-  
26 1989.  
27  
28  
29 57. Vlahos CJ, Matter WF, Hui KY and Brown RF A specific inhibitor of  
30 phosphatidylinositol-3-kinase, 2-(4-morpholinyl)-8-phenyl-4H-1-benzopyran-4-one  
31 (LY294002). J Biol Chem 1994; 269: 5241-5248.  
32  
33  
34 58. Goettert M, Schattel V, Koch P, Merfort I and Laufer S Biological evaluation and  
35 structural determinants of p38 $\alpha$  mitogen-activated-protein kinase and c-Jun-N-terminal  
36 kinase 3 inhibition by flavonoids. Chembiochem 2010; 11: 2579-2588.  
37  
38  
39 59. Hwang MK, Kang NJ, Heo YS, Lee KW, Lee HJ Fyn kinase is a direct molecular target  
40 of delphinidin for the inhibition of cyclooxygenase-2 expression induced by tumor  
41 necrosis factor-alpha. Biochem Pharmacol 2009; 77: 1213-1222.  
42  
43  
44 60. Traxler P, Green J, Mett H, Sequin U, Furet P Use of a pharmacophore model for the  
45 design of EGFR tyrosine kinase inhibitors: isoflavones and 3-phenyl-4(1H)-quinolines. J  
46 Med Chem 1999; 42: 1018-1026.  
47  
48  
49 61. Lambert C, Leonard N, De Bolle X, Depiereux E ESyPred3D: Prediction of proteins 3D  
50 structures. Bioinformatics 2002; 18: 1250-1256.  
51  
52  
53  
54  
55  
56  
57  
58  
59  
60  
61  
62  
63  
64  
65

1  
2  
3  
4  
5  
6  
7  
8  
9  
10  
11  
12  
13  
14  
15  
16  
17  
18  
19  
20  
21  
22  
23  
24  
25  
26  
27  
28  
29  
30  
31  
32  
33  
34  
35  
36  
37  
38  
39  
40  
41  
42  
43  
44  
45  
46  
47  
48  
49  
50  
51  
52  
53  
54  
55  
56  
57  
58  
59  
60  
61  
62  
63  
64  
65

62. McGuffin LJ The ModFOLD server for the quality assessment of protein structural models. *Bioinformatics* 2008; 24: 586-587.

63. McGuffin LJ Prediction of global and local model quality in CASP8 using the ModFOLD server. *Proteins-Structure Function and Bioinformatics* 2009; 77: 185-190.

64. Pastor M and Cruciani G A novel strategy for improving ligand selectivity in receptor-based drug design. *J Med Chem* 1995; 38: 4637-4647.

## Figure Legend

### Figure 1. **Flavonoid structures.**

The flavonoid structure comprises an oxygenated heterocyclic middle ring (C ring) flanked by 2 aromatic rings (A and B rings). Flavones (apigenin) are characterised by a non-hydroxylated C ring, whereas flavonol (quercetin) C rings contain a C-10 hydroxyl group. Flavan-3-ols (catechin) are defined by a non-planar, C-10 hydroxylated C ring that is not substituted with a C-9 carbonyl group.

### Figure 2. **Structural alignments of Lyn, Fyn and Hck kinase domains.**

The Dali-lite structural sieving server was used to perform structural alignments of Hck (2HCK), Lyn (3A4O) and Fyn (2DQ7) kinase domains. The RMSD for Hck and Lyn was 2 Å, for Hck and Fyn was 1.9 Å, and for Lyn and Fyn was 1.2Å.

### Figure 3. **Homology models built for Lyn tyrosine kinase (Homo sapiens).**

Homology model of human Lyn kinase, based on the 2H8H template, using the ESyPred3D server [61] (A). The per-residue error was predicted using the ModFOLD server [40, 63-64]. The colours represent the residue accuracy according to a pseudo-temperature scheme (blue indicates residues closest to the native structure; red, those furthest from the native structure). Superimposition (performed using Mustang-MR) of the homology model of Lyn kinase domain (blue), from the 2H8H template, and the X-ray crystal structure of human Lyn kinase domain (green, PDB-ID 3A4O) (B). The RMSD between the kinase domains of the homology model and the crystal structure using Dalilite was 1.6 Å. Superimposition of the active site of Lyn kinase domain homology model (blue) and Lyn kinase domain crystal structure (green) (C). Active site residues are highlighted as ball and stick. Reference [61] refers to the use of the methods developed by the authors of the cited publication.

### Figure 4. **The active site of Hck kinase domain (PDB-ID 2HCK) containing co-crystallised and docked quercetin molecules.**

1  
2  
3  
4 An electrostatic surface representation of the homology model of the Lyn kinase domain showing  
5 docked quercetin (A) and Hck kinase domain (2HCK) containing co-crystallised (dark blue) and  
6 docked (light blue) quercetin (B). ). The RMSD between docked and crystallised quercetin  
7  
8 molecules was 1.6 Å.  
9

10  
11  
12  
13 **Figure 5. Molecular docking and interaction energies of flavonoids in the substrate binding**  
14 **groove of the modelled Lyn kinase domain.**  
15

16 The docked ligands (quercetin: A, B; apigenin: C, D; catechin: E, F) are shown in bold outline  
17 with neighbouring amino acid residues indicated. Hydrogen bonds (depicted by dashed lines) are  
18 shown between the ligand and active site residues with the bond lengths given in Angstroms (Å).  
19 The GRID programme predicted three dimensional energy contour surfaces/regions (dotted areas  
20 around docked ligands – quercetin: B; apigenin: D; catechin: F) within the ATP binding groove  
21 of the Lyn model corresponding to the energy minima of hydrophilic (OH: grey dotted areas) and  
22 hydrophobic (DRY: black dotted areas), which act as small chemical probes representative of  
23 flavonoid functional groups (OH: hydroxyl groups and DRY: aromatic groups). GRID showed  
24 areas of hydrophilic interactions (GLY344 and the C ring C-10 hydroxyl) corresponding to the  
25 hydrogen bonds formed by quercetin. The A ring C-6 hydroxyl on the structure of apigenin,  
26 forming hydrogen bonds with MET91 and GLU89, was adjacent to hydrophilic GRID regions.  
27 GRID hydrophilic interactions correspond to hydrogen bonds formed between GLU89, MET91  
28 and ALA92, and the A and B ring hydroxyl oxygens on the structure of catechin.  
29  
30  
31  
32  
33  
34  
35  
36  
37  
38  
39  
40  
41  
42  
43

44 **Figure 6. Flavonoids block the kinase activity of Hck and Lyn**  
45

46 Washed human platelets ( $8 \times 10^8$  cells.mL<sup>-1</sup>) in the presence of EGTA (1 mM) were stimulated  
47 with collagen (25 µg.mL<sup>-1</sup>) for 90 s. Platelets were lysed with ice-cold 1% NP40 and Lyn was  
48 immunoprecipitated. Lyn immunoprecipitates and recombinant Hck were pre-treated with  
49 flavonoids (quercetin, catechin or apigenin), or solvent control (DMSO (0.2% v/v)) for 5 min.  
50 Immunoprecipitates were assayed for kinase activity (see Materials and Methods). Equivalent  
51 protein loading was verified by reprobing for Lyn and silver staining Hck protein. % inhibition of  
52 kinase activity is a percentage of the DMSO-treated, collagen-stimulated control (0% inhibition).  
53 The bars represent the mean (n = 3) % inhibition of kinase activity for each treatment (± S.E.M).  
54  
55  
56  
57  
58  
59  
60  
61  
62  
63  
64  
65

1  
2  
3  
4 \*  $P \leq 0.05$ , \*\*  $P \leq 0.01$  and \*\*\*  $P \leq 0.001$  compared to the control (DMSO-treated, collagen-  
5 stimulated platelets).  
6  
7  
8  
9

10  
11 **Supplemental Figure 1. Molecular docking and GRID interaction energies of flavonoids in**  
12 **the ATP binding site of the Hck kinase domain.**  
13

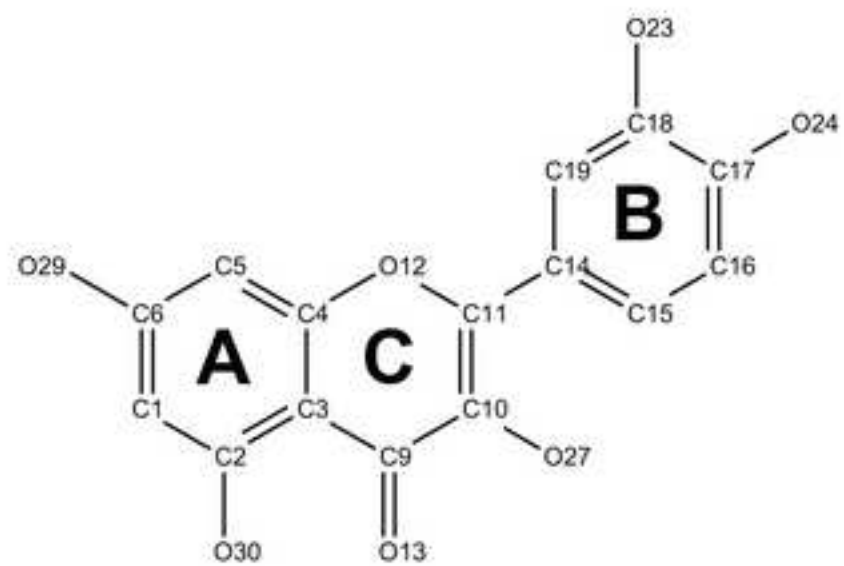
14  
15 The docked ligands (quercetin: A, B; apigenin: C, D; catechin: E, F) are shown in bold outline  
16 with neighbouring amino acid residues indicated. Hydrogen bonds (depicted by dashed lines) are  
17 shown between the ligand and binding site residues with the bond lengths given in Angstroms  
18 ( $\text{\AA}$ ). The GRID programme predicted three dimensional energy contour surfaces/regions (dotted  
19 areas around docked ligands – quercetin: B; apigenin: D; catechin: F) within the substrate binding  
20 groove of the Hck kinase domain (crystal structure) corresponding to the energy minima of  
21 hydrophilic (OH: grey dotted areas) and hydrophobic (DRY: black dotted areas) small chemical  
22 probes representative of flavonoid functional groups (OH: hydroxyl groups and DRY: aromatic  
23 groups). MET85 as well as the hydrogen bond contacts formed between ASP148 and LYS39 and  
24 quercetin B ring hydroxyls were surrounded by hydrophilic GRID regions. Apigenin hydrogen  
25 bonds (A ring C-6 hydroxyl) to ASN19 as well as the THR82 and GLU83 bound to the apigenin  
26 B ring C-4' hydroxyl are near hydrophilic GRID areas. MET85 and catechin C ring C-10  
27 hydroxyls are also adjacent to GRID hydrophilic areas.  
28  
29  
30  
31  
32  
33  
34  
35  
36  
37  
38  
39  
40  
41  
42

43 **Supplemental Figure 2. Molecular docking and GRID interaction energies of flavonoids in**  
44 **the ATP binding site of the Fyn kinase domain.**  
45

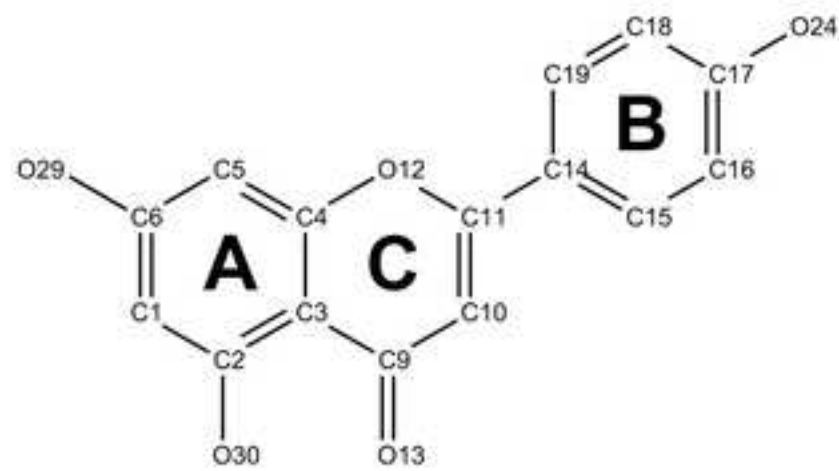
46 The docked ligands (quercetin: A, B; apigenin: C, D; catechin: E, F) are shown in bold outline  
47 with neighbouring amino acid residues numbered. Hydrogen bonds (depicted by dashed lines) are  
48 shown between the ligand and binding site residues with the bond lengths given in Angstroms  
49 ( $\text{\AA}$ ). The GRID programme predicted three dimensional energy contour surfaces/regions (dotted  
50 areas around docked ligands – quercetin: B; apigenin: D; catechin: F) within the substrate binding  
51 groove of the Fyn kinase domain (crystal structure) corresponding to the energy minima of  
52 hydrophilic (OH: grey dotted areas) and hydrophobic (DRY: black dotted areas) small chemical  
53 probes representative of flavonoid functional groups (OH: hydroxyl groups and DRY: aromatic  
54 groups).  
55  
56  
57  
58  
59  
60  
61  
62  
63  
64  
65

1  
2  
3  
4 groups). GRID areas of hydrophilic interactions were between the quercetin C ring C-10  
5 hydroxyl and GLY344. MET341 binding to A ring C-6 hydroxyl and SER345 and ASP348  
6 hydrogen bonds to the B ring C-17 hydroxyl on the structure of apigenin are also adjacent to  
7 hydrophilic interactions. MET341, ALA342 and LEU273 and C and A ring hydroxyls on the  
8 structure of catechin are near hydrophilic GRID regions.  
9  
10  
11  
12  
13  
14  
15  
16  
17  
18  
19  
20  
21  
22  
23  
24  
25  
26  
27  
28  
29  
30  
31  
32  
33  
34  
35  
36  
37  
38  
39  
40  
41  
42  
43  
44  
45  
46  
47  
48  
49  
50  
51  
52  
53  
54  
55  
56  
57  
58  
59  
60  
61  
62  
63  
64  
65

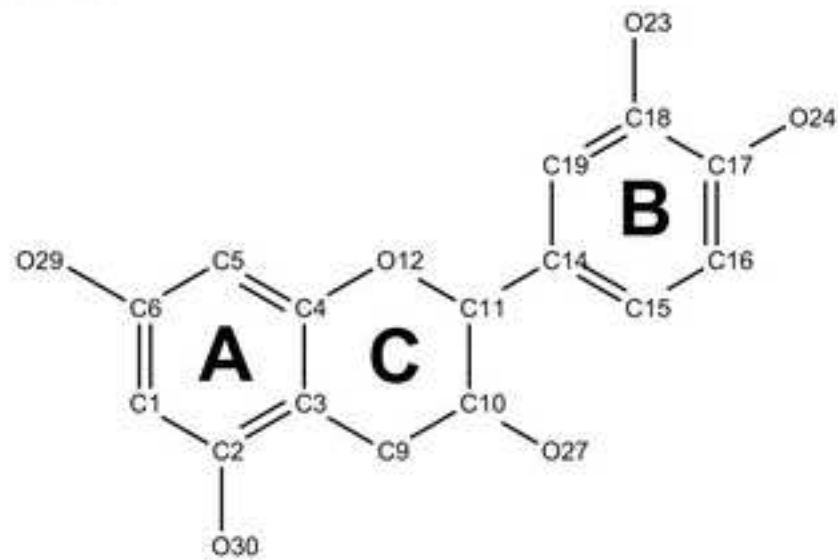
Figure 1  
[Click here to download high resolution image](#)



quercetin



apigenin



catechin

Figure 2

[Click here to download high resolution image](#)

**A**

Hck	KDAWEIPRESLKLKLEKLGAGQFGGEVWIGATYNNKHTKVAVKTKPGSMVEAPLAEANVMKT	60
Lyn	.DAWEIPRESIKLVKRLGAGQFGGEVWIGYNNSTKVAVKTLKPGTMSVQAPLAEANLMKT	59
Hck	LQHDKLVKLVAVVTK.EPIYIIITEFMANGSLLDFLKSDGEGSKQPLPKLIDFSAQIAEGMA	119
Lyn	LQHDKLVRLYAVVTRQEPYIIITEFMANGSLLDFLKSDGEGKVLPLKIDFSAQIAEGMA	119
Hck	FIEQRNYINPDLRAANILVVSASLVCKIADFGL.arvgakFPKNTAPEAINFGSFTIKSD	178
Lyn	YIERKNYINPDLRAANVLVSESLMCKIADFGLARvegakFPKNTAPEAINFGCFTIKSD	179
Hck	VNSFGILLMEIVTYGRIPYPMNSPEVIRALERGYRMPRPENCPEELYNIMRCCKNRPE	238
Lyn	VNSFGILLYEIVTYGKIPYPRGTNADVMTALSQGYRMPRVENCPEDELYDIMRCCKEKAE	239
Hck	ERPTFEYIQSVLDD.FYTatesq	260
Lyn	ERPTFDYLQSVLDDFYTAT...e	259

**B**

Hck	KDAWEIPRESLKLKLEKLGAGQFGGEVWIGATYNNKHTKVAVKTKPGSMVEAPLAEANVMKT	60
Fyn	KDVWEIPRESLQLIKRLGNGQFGGEVWIGTWNKTKVAIKTLKPGTMSPEFLAEQIMNK	60
Hck	LQHDKLVKLVAVVTKQEPYIIITEFMANGSLLDFLKSDGEGSKQPLPKLIDFSAQIAEGMAF	120
Fyn	LGHDKLVQLYAVVSEEPYIIVTEIDKNGSLLDFLKDGEGRALKLPLNLDVMAAQVAAGMAY	120
Hck	IEQRNYIHRDLRAANILVVSASLVCKIADFGL.....arvgakFPKNTAPEAINFG	171
Fyn	IERNYIHRDLRSANILVGNGLICKIADFGLARLiednetarqgAKFPKNTAPEAALYQ	180
Hck	SFTIKSDVNSFGILLMEIVTYGRIPYPMNSPEVIRALERGYRMPRPENCPEELYNIMRC	231
Fyn	RFTIKSDVNSFGILLTELVTGRVYPPGQSNREVLEQVERGYRMPCPQDCPISLHELMIH	240
Hck	CKNRPEERPTFEYIQSVLDDFytatesq	260
Fyn	CKNKDPEERPTFEYLQSFLEDY.....	262

**C**

Lyn	.DAWEIPRESIKLVKRLGAGQFGGEVWIGYNNSTKVAVKTLKPGTMSVQAPLAEANLMKT	59
Fyn	KDVWEIPRESLQLIKRLGNGQFGGEVWIGTWNKTKVAIKTLKPGTMSPEFLAEQIMNK	60
Lyn	LQHDKLVRLYAVVTRQEPYIIITEFMANGSLLDFLKSDGEGKVLPLKIDFSAQIAEGMA	119
Fyn	LKHDKLVQLYAVVSE.EPIYIVTEFMANGSLLDFLKDGEGRALKLPLNLDVMAAQVAAGMA	119
Lyn	YIERKNYINPDLRAANVLVSESLMCKIADFGLARV.....EGAKFPKNTAPEAIN	170
Fyn	YIERQNYINPDLRSANILVGNGLICKIADFGLARLiednetarqGAKF.PKNTAPEAAL	178
Lyn	FGCFTIKSDVNSFGILLYEIVTYGKIPYPRGTNADVMTALSQGYRMPRVENCPEDELYDIM	230
Fyn	YGRFTIKSDVNSFGILLTELVTGRVYPPGQSNREVLEQVERGYRMPCPQDCPISLHEIM	238
Lyn	RCCKEKAEERPTFDYLQSVLDDFytate	259
Fyn	INCKKDPEERPTFEYLQSFLEDY.....	262

Figure 3  
[Click here to download high resolution image](#)

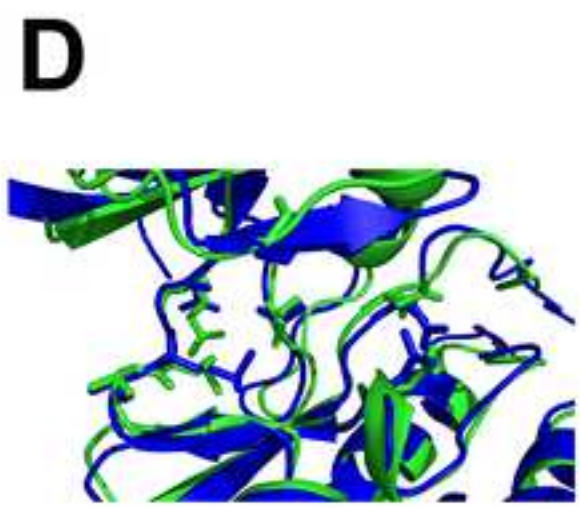
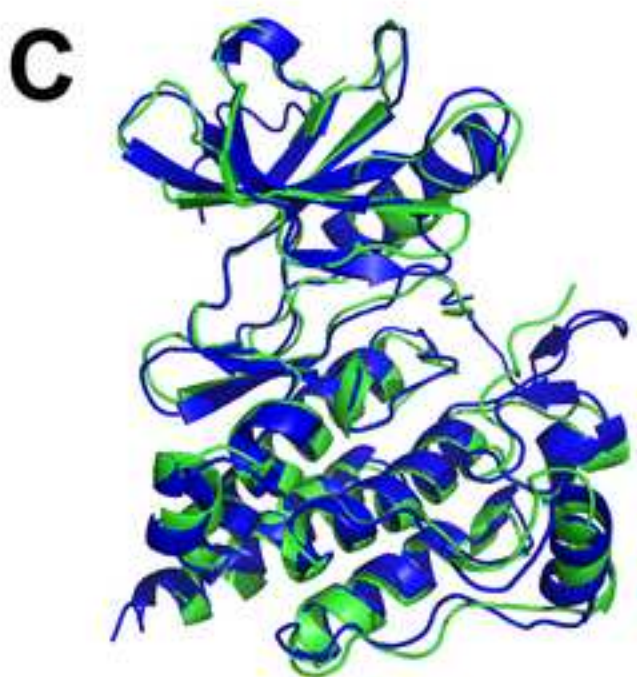
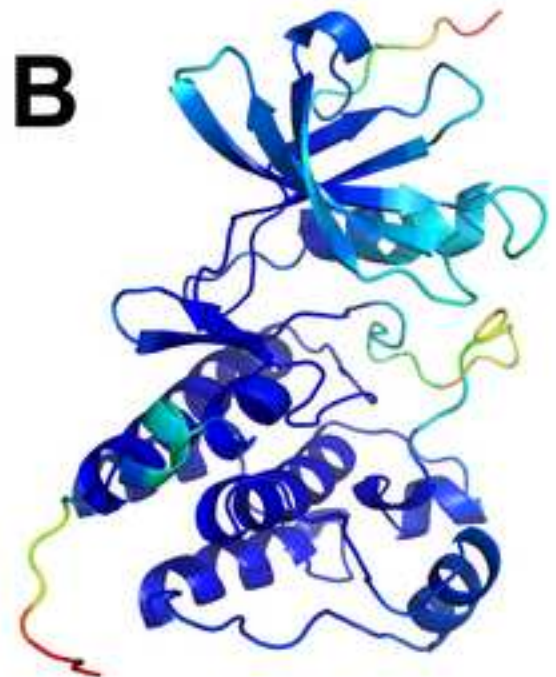
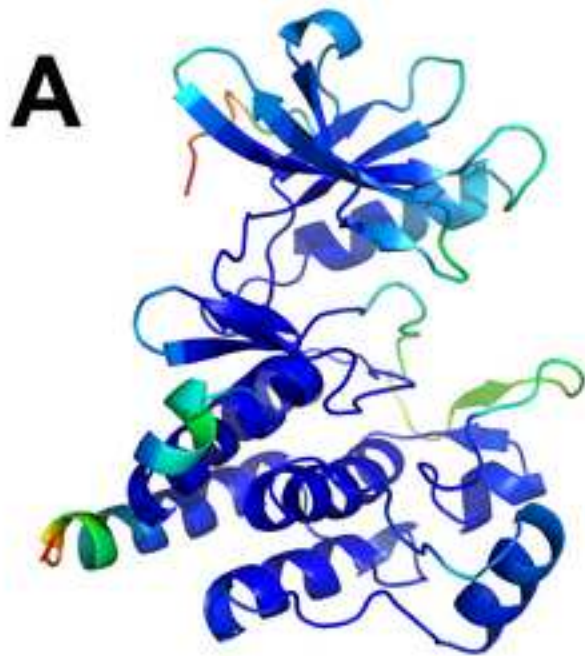


Figure 4  
[Click here to download high resolution image](#)

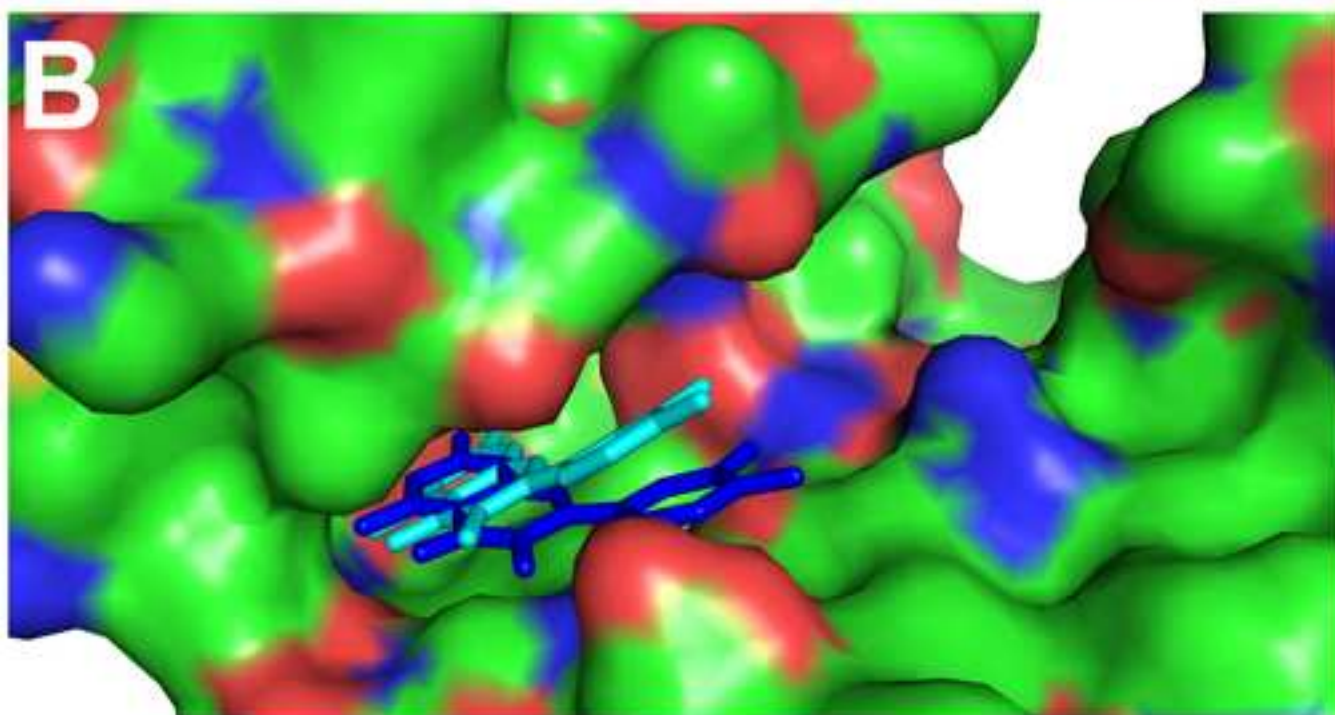
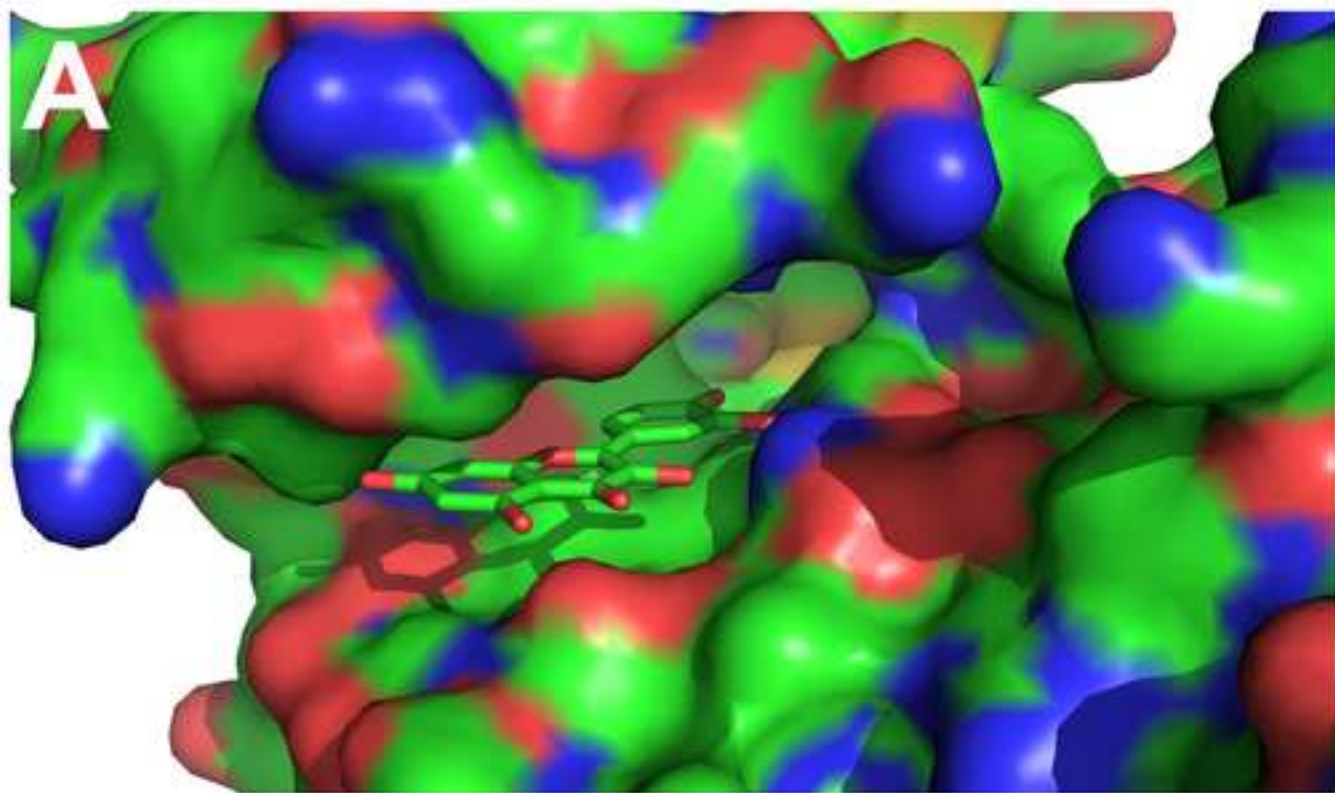


Figure 5  
[Click here to download high resolution image](#)

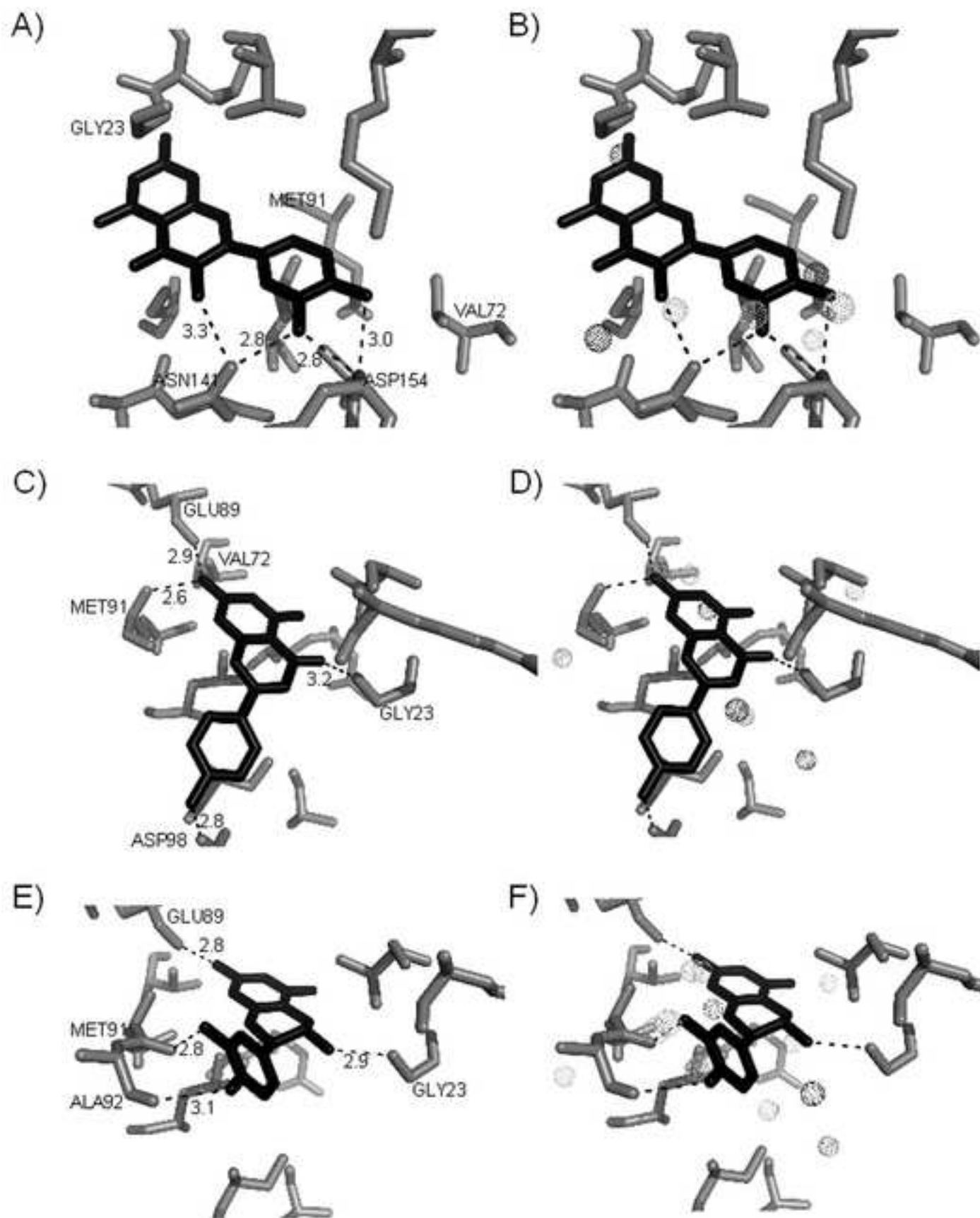
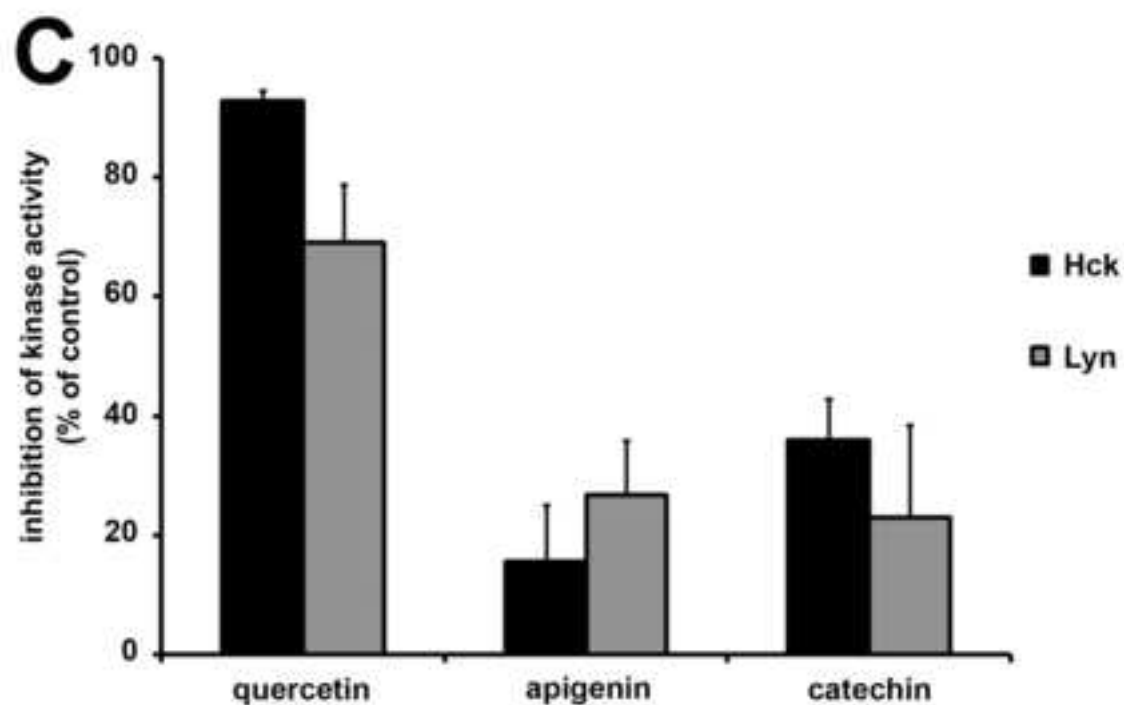
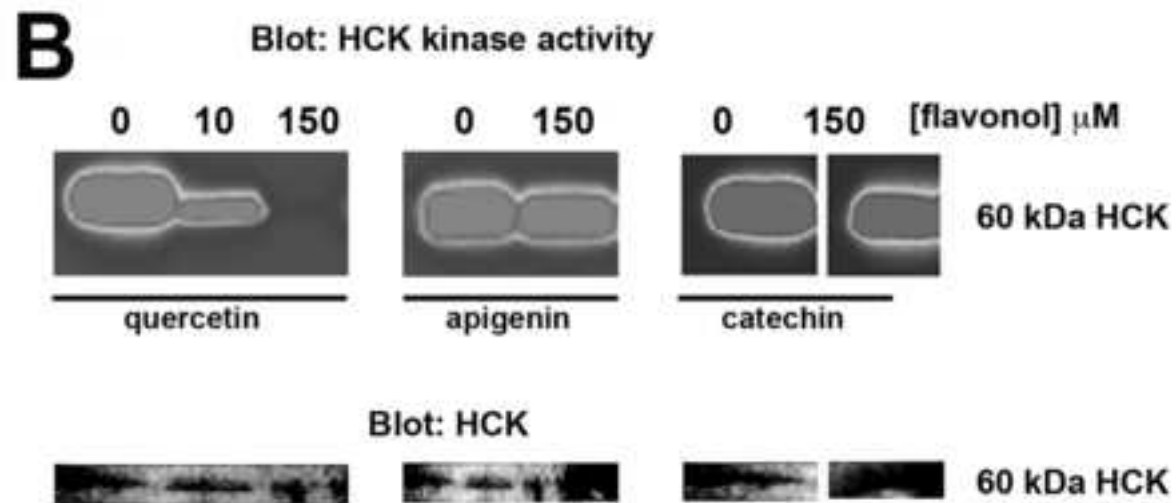
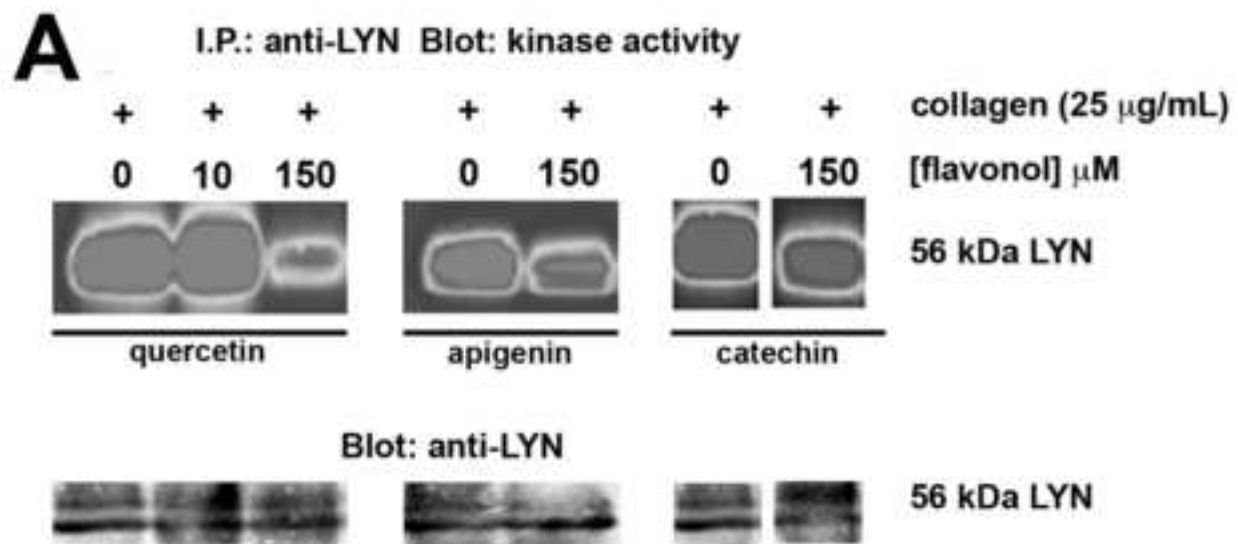


Figure 6

[Click here to download high resolution image](#)



**Supplemental Figure 1**

[Click here to download Supplemental file for online publication: Supplemental\\_Figure\\_1.png](#)

**Supplemental Figure 2**

[Click here to download Supplemental file for online publication: Supplemental\\_Figure\\_2.png](#)